Inorg. Chem. **2002**, *41*, 4509–4523

Reactions of a Ruthenium(II) Arene Antitumor Complex with Cysteine and Methionine

Fuyi Wang, Haimei Chen, John A. Parkinson, Piedad del Socorro Murdoch, and Peter J. Sadler*

Department of Chemistry, University of Edinburgh, King's Buildings, West Mains Road, Edinburgh EH9 3JJ, U.K.

Received February 13, 2002

The Ru(II) organometallic antitumor complex [(η^6-biphenyl)RuCl(en)][PF_6] (**1**) reacts slowly with the amino acid L-cysteine (L-$CysH_2$) in aqueous solution at 310 K. Reactions were followed over periods of up to 48 h using HPLC, electronic absorption spectroscopy, LC-ESI-MS, and 1D or 2D ^{1}H and ^{15}N NMR spectroscopy. Reactions at a 1 mM/2 mM (Ru/L-$CysH_2$) ratio were multiphasic in acidic solutions (pH 5.1) and appeared to involve aquation as the first step. Initially, 1:1 adducts involving substitution of Cl by S-bound or O-bound L-$CysH_2$, [(η^6-biphenyl)Ru(*S*-L-CysH)(en)]$^+$ (**4a**) and [(η^6-biphenyl)Ru(*O*-L-$CysH_2$)(en)]$^{2+}$ (**4b**) formed, followed by the cystine adduct [(η^6-biphenyl)-Ru(*O*-Cys_2H_2)(en)]$^{2+}$ (**3**), and two dinuclear complexes from which half or all of the chelated ethylenediamine had been displaced, [(η^6-biphenyl)Ru(H_2O)(μ*S*,*N*-L-Cys)Ru(η^6-biphenyl)(en)]$^{2+}$ (**5**) containing one bridging cysteine, and [(η^6-biphenyl)Ru(*O*,*N*-L-Cys-*S*)(*S*-L-Cys-*N*)Ru(η^6-biphenyl)(H_2O)] (**6**) containing two bridging cysteines. The unusual cluster species {(biphenyl)Ru}$_8$ (**7a**) was also detected by MS and was more prevalent in reactions at higher L-$CysH_2$ concentrations. Complex **5** was the dominant product at pH 2–5, but overall, only ca. 50% of **1** reacted with L-$CysH_2$ in these conditions. The reaction between **1** and L-$CysH_2$ was suppressed in 50 mM triethylammonium acetate solution at pH > 5 or in 100 mM NaCl. Only 27% of complex **1** reacted with L-methionine (L-MetH) at an initial pH of 5.7 after 48 h at 310 K and gave rise to only one adduct [(η^6-biphenyl)Ru(*S*-L-MetH)(en)]$^{2+}$ (**8**).

Introduction

Ruthenium arene complexes are known to have antibacterial activity[1] and have the potential for inhibiting enzymes involved in DNA biochemistry.[2] Recently, we have shown that Ru(II) arene complexes of the type [(η^6-arene)Ru(X)-(YZ)] where X is a leaving group such as Cl^-, and YZ is a chelating diamine such as ethylenediamine (en), are cytotoxic to cancer cells including cisplatin-resistant cell lines.[3] An example is [(η^6-biphenyl)RuCl(en)][PF_6] (**1**), a stable, water-soluble complex with the characteristic "piano-stool" structure, which is active in the A2780 human ovarian cancer xenograft and non-cross-resistant in the A2780cis xenograft.[4] Such complexes appear to bind strongly and specifically to guanine bases on DNA,[5] and DNA may be an important target site for this class of cytotoxic agents. Recently, related phosphine adducts such as [(η^6-*p*-cymene)$RuCl_2$(pta)] (pta = 1,3,5-triaza-7-phosphatricyclo[3.3.1.1]decane) have been shown to be active.[6] Additional interest in the biological chemistry of Ru complexes arises from, for example, clinical trials of NAMI-A as an antimetastatic agent[7] and the activity of related complexes containing heterocyclic nitrogen ligands.[8]

Most metal complexes can readily undergo ligand substitution reactions and, in the case of transition metals, sometimes also redox reactions. The role of these in the biological activity of metal complexes depends both on their

* To whom correspondence should be addressed. E-mail: p.j.sadler@ed.ac.uk. Fax: +44 131 650 6452.

(1) Çetinkaya, B.; Özdemir, I.; Binbasioglu, B.; Durmaz, R.; Günal, S. *Arzneim.-Forsch.* **1999**, *49* (I), 538−540.
(2) Gopal, Y. N. V.; Jayaraju, D.; Kondapi, A. K. *Biochemistry* **1999**, *38*, 4382−4388.
(3) (a) Morris, R. E.; Aird, R. E.; Murdoch, P. del S.; Chen, H.; Cummings, J.; Hughes, N. D.; Parsons, S.; Parkin, A.; Boyd, G.; Jodrell, D. I.; Sadler, P. J. *J. Med. Chem.* **2001**, *44*, 3616−3621. (b) Cummings, J.; Aird, R. E.; Morris, R. E.; Chen, H.; Murdoch, P. del S.; Sadler, P. J.; Smyth, J. F.; Jodrell, D. I. *Clin. Cancer Res.* **2000**, *6*, 142.
(4) Aird, R. E.; Cummings, J.; Ritchie, A. A.; Muir, M.; Morris, R. E.; Chen, H.; Sadler, P. J.; Jodrell, D. I. *Br. J. Cancer* **2002**, *86*, 1652−1657.
(5) Chen, H.; Parkinson, J. A.; Parsons, S.; Coxall, R. A.; Gould, R. O.; Sadler, P. J. *J. Am. Chem. Soc.* **2002**, *124*, 3064−3082.
(6) (a) Allardyce, C. S.; Dyson, P. J.; Ellis, D. J.; Heath, S. L. *Chem. Commun.* **2001**, 1396−1397. (b) Allardyce, C. S.; Dyson, P. J. *Platinum Metals Rev.* **2001**, *45* (2), 62−69.
(7) Sava, G.; Gagliardi, R.; Bergamo, A.; Alessio, E.; Mestroni, G. *Anticancer Res.* **1999**, *19*, 969−972.
(8) Peti, W.; Piueper, T.; Sommer, M.; Keppler, B. K.; Giester, G. *Eur. J. Inorg. Chem.* **1999**, 1551−1555.

10.1021/ic025538f CCC: $22.00
Published on Web 07/26/2002

Chart 1. Schematic Drawings of Complex **1** and Its Adducts with H_2O (**2a**), TFA (**2b**), Cystine (**3**), and L-Cysteine (**4a** and **4b**)

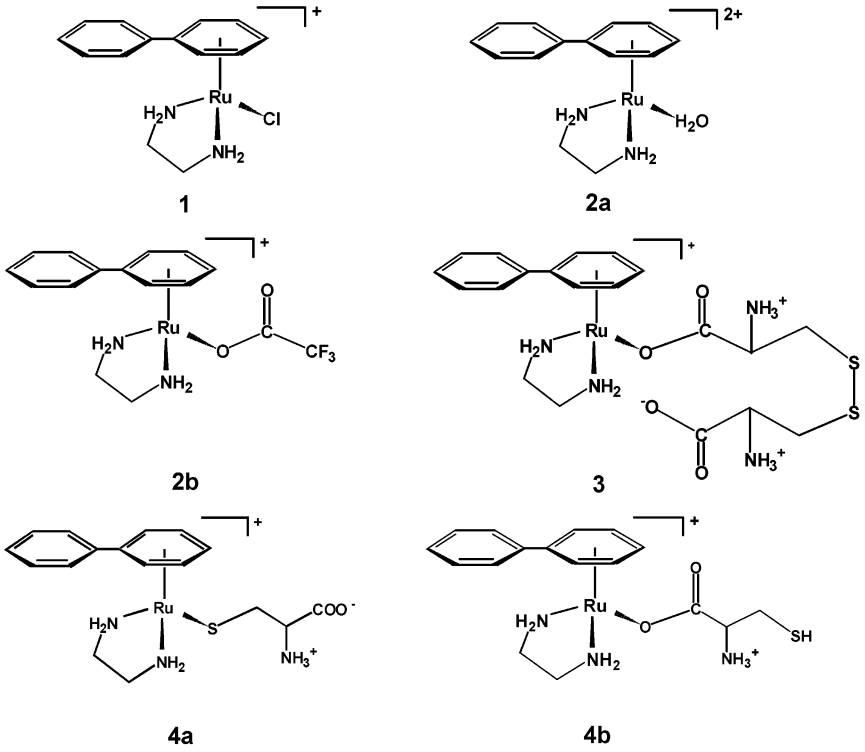

extent (thermodynamics) and on the rate (kinetics). It is therefore of interest to investigate reactions between candidate metallodrugs and biomolecules in order to understand both in vitro and in vivo biological data. The metal complex may undergo a chemical transformation in the cell culture medium, or in blood plasma, or in the cell membrane or cytoplasm before it reaches the target site (e.g., DNA in the nucleus or mitochondrion).

Reactions with the sulfur-containing amino acids L-cysteine (L-$CysH_2$) and L-methionine (L-MetH) appear to play key roles in the biological chemistry of both Pt(II) and Pt(IV), and Ru(III) anticancer agents. The concentration of the cysteine-containing tripeptide glutathione is elevated in some platinum-resistant cell lines, and thiols appear to be involved in the reduction of Pt(IV) and Ru(III) complexes to active Pt(II) and Ru(II) species.[9,10] Methionine adducts of cisplatin and carboplatin have been detected in animal urine.[11]

In this work, we have used a combination of high performance liquid chromatography (HPLC), electronic absorption spectroscopy, electrospray ionization mass spectrometry (ESI-MS), and nuclear magnetic resonance (NMR) spectroscopy to investigate the structures of products from reactions of the ruthenium(II) arene anticancer complex [(η^6-biphenyl)RuCl(en)][PF_6] (**1**) with L-cysteine and L-methionine in aqueous solution. The reaction of complex **1** with L-cysteine afforded six novel adducts, three mononuclear complexes (**3**, **4a**, **4b**), one singly bridged dinuclear adduct (**5**), and one doubly bridged dinuclear adduct (**6**) (Charts 1 and 2). In the presence of high concentrations of L-cysteine, an unusual ruthenium cluster species (**7a**) was also detected. In contrast, reactions of complex **1** with L-methionine followed a single pathway giving the mononuclear adduct **8** (Chart 3).

Experimental Section

Materials. [(η^6-biphenyl)RuCl(en)][PF_6] (**1**) and ^{15}N-labeled **1** (^{15}N-**1**) were synthesized as described elsewhere.[3] L-Cysteine, L-methionine, and triethlyammonium acetate (TEAA, 1.0 M) were purchased from Fluka, and trifluoroacetic acid (TFA) was purchased from Arcos.

Ultraviolet and Visible (UV−Vis) Spectrometry. A Perkin-Elmer Lambda-20 UV−vis recording spectrophotometer was used with 1 cm path-length quartz cuvettes (0.5 mL) and a PTP1 Peltier temperature controller. Spectra were processed with UVWinlab software for Windows 95.

High Performance Liquid Chromatography (HPLC). A Hewlett-Packard series 1100 quaternary pump and a Rheodyne sample injector with 100 μL and 2.0 mL loops, an HP 1100 series UV−vis detector, and an HP 1100 series Chemstation with an HP enhanced integrator were used. Analytical separations were carried out on a PLRP-S reversed-phase column (250 mm × 4.6 mm, 100 Å, 5 μm, Polymer Labs), and semipreparative work was carried out on a Lichrosorb 5RP18 reversed-phase column (250 mm × 8 mm, 5 μm, Technicol Ltd.) with detection at 254 nm. Mobile phase A: water (purified using a Millipore Elix 5 system) containing 0.1%

(9) (a) Talman, E. G.; Brüning, W.; Reedijk, J.; Spek, A. L.; Veldman, N. *Inorg. Chem.* **1997**, *36*, 854−861. (b) Kratochwil, N. A.; Guo, Z.; Murdoch, P. del S.; Parkinson, J. A.; Bednarski, P. J.; Sadler, P. J. *J. Am. Chem. Soc.* **1998**, *120*, 8253−8254.

(10) (a) Mestroni, G.; Alessio, E.; Sava, G.; Pacor, S.; Coluccia, M.; Boccarelli, A. *Met.-Based Drugs* **1994**, *1*, 41−63. (b) Mestroni, G.; Alessio, E.; Sava, G.; Pacor, S.; Coluccia, M. In *Metal Complexes in Cancer Chemotherapy*; Keppler, B. K., Ed.; VCH: Weinheim, 1993. (c) Clarke, M. J.; Zhu, F.; Frasca, D. R. *Chem. Rev.* **1999**, *99*, 2511−2533. (d) Frasca, D. R.; Clarke, M. J. *J. Am. Chem. Soc.* **1999**, *121*, 8523−8532.

(11) (a) Riley, C. M.; Sternson, L. A.; Repta, A. J.; Slyter, S. A. *Anal. Biochem.* **1983**, *130*, 203−214. (b) Barnham, K. J.; Frey, U.; Murdoch, P. del S.; Ranford, J. D.; Sadler, P. J. *J. Am. Chem. Soc.* **1994**, *116*, 11175−11176.

Chart 2. Schematic Drawings of Di-Ruthenium Complexes **5** and **6**, Products from Reaction of Complex **1** with L-Cysteine (Some Protons Omitted for Clarity)[a]

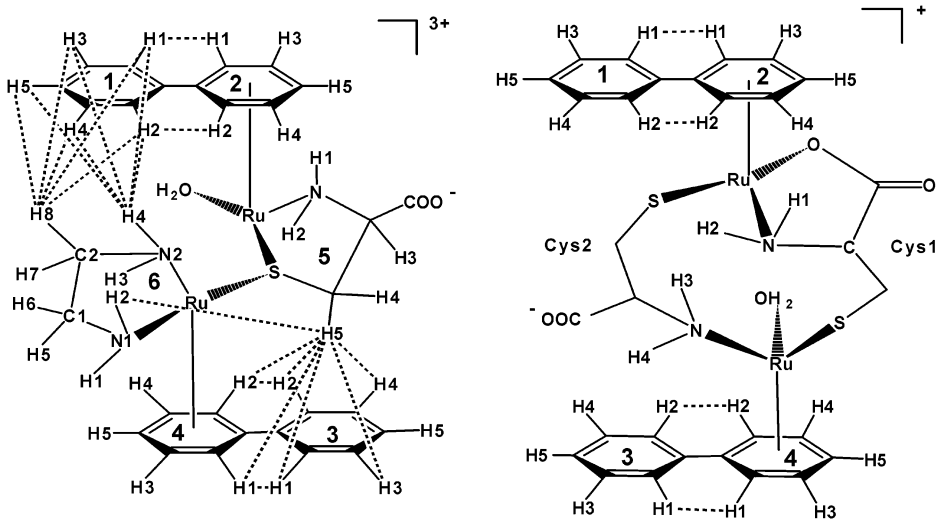

5 **6**

[a] The dotted lines indicate observed NOEs. The NOEs between H61, H63 (protons in ring 6) and H41−H45 (protons in ring 4) of complex **5** were not resolvable because of overlap of cross-peaks with NOEs between aromatic protons H41−H45.

Chart 3. Schematic Drawing of Adduct **8**, Product from Reaction of Complex **1** with L-Methionine

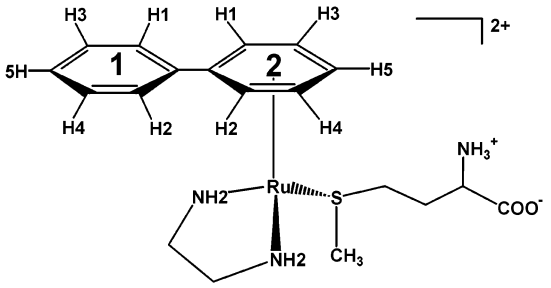

8

TFA. Mobile phase B: acetonitrile (for HPLC application, Fisher Chemicals) containing 0.1% TFA. For analytical assays, the flow rate was 1.0 mL min^{-1}, for semipreparative work, 4 mL min^{-1}. The gradient (solvent B) was the following: 2% from 0 to 5 min, 15% from 6 to 15 min, 26.5% from 18 to 30 min, 60% from 32 to 35 min, and resetting to 2% at 40 min. For the semipreparative work, the gradient over 18 to 30 min was changed from 26.5% to 23.0%.

Electrospray Ionization Mass Spectroscopy (ESI-MS). Positive-ion electrospray ionization mass spectra were obtained with a Platform II mass spectrometer (Micromass, Manchester, U.K.). For offline ESI-MS assays, the samples were prepared with a 50% CH_3CN/50% H_2O mixture and infused at 8 μL min^{-1} directly into the mass spectrometer, and the ions were produced in an atmospheric pressure ionization (API)/ESI ion source. For the online LC-ESI-MS assays, a Waters 2690 HPLC system was interfaced with the mass spectrometer, using the same column and gradients as described previously for the analytical HPLC assays with a flow rate of 1.0 mL min^{-1} and a splitting ratio of 1/6. The spray voltage was 3.50−3.68 kV. The cone voltage was varied over the range 15−60 V as required. The capillary temperature was 338 K for direct infusion and 373 K for the HPLC sampling, with a 450 L h^{-1} flow of nitrogen drying gas. The quadrupole analyzer, operated at a background pressure of 2×10^{-5} Torr, was scanned at 300 Da s^{-1} for direct infusion and 900 Da s^{-1} for HPLC sampling. Data were collected (for 10 scans during the direct infusion assays) and analyzed on a Mass Lynx (ver. 2.3) Windows NT PC data system using the Max Ent Electrospray software algorithm and calibrated versus an NaI calibration file. The mass accuracy of all measurements was within 0.1 m/z unit. For the instrument used, the resolution, as calculated from $m/\Delta m_{50\%}$, where $\Delta m_{50\%}$ is the width of the mass spectral peak at half-height, ranges from 524.8 at m/z = 314.9 to 1340 at m/z = 803.9.

Nuclear Magnetic Resonance (NMR) Spectroscopy. (a) For HPLC-isolated adducts, NMR data were acquired at a temperature of 298 K using a Varian ^{Unity}INOVA 600 MHz NMR spectrometer equipped with a triple resonance (^{1}H, ^{13}C, ^{15}N) z-gradient probehead.

1D ^{1}H NMR data were acquired with 128 transients into 64K data points over a frequency width of 7 kHz using a double pulsed-field gradient spin−echo routine (DPFGSE) to eliminate the solvent resonance.[12] A relaxation delay of 2 s was applied between transients.

2D ^{1}H DQFCOSY, TOCSY, NOESY, and ROESY NMR data were acquired over a frequency width of 7 kHz in both F2 and F1 into 4K complex data points in F2 (acquisition time = 293 ms) with 32 transients for each of 2×300 t_1 increments. A relaxation delay of 2 s between transients was used for all experiments. Specifically, two 2D NOESY NMR data sets were acquired with mixing times of 500 ms and 1 s. Water suppression was achieved using a DPFGSE routine after the final read pulse. The 2D TOCSY NMR data were acquired with a spin-lock time of 75 ms. The water resonance was suppressed by means of a DPFGSE routine. 2D ROESY NMR data were acquired with a mixing time of 150 ms with solvent suppression achieved using a DPFGSE routine. 2D DQFCOSY data were acquired using a pulse program based on that of Altieri and Byrd[13] in which the solvent resonance is eliminated by combining water randomization at the start of the pulse sequence with a composite WATERGATE sequence prior to data acquisition in order to reduce dispersive tails on cross-peaks.

(12) Hwang, T. L.; Shaka, A. J. *J. Magn. Reson., Ser. A* **1995**, *112*, 275−279.
(13) Altieri, A. S.; Byrd, R. A. *J. Magn. Reson., Ser. B* **1995**, *107*, 260−266.

Data were processed using standard apodizing functions prior to Fourier transformation.

(b) The time course of the reaction between ^{15}N-**1** and L-cysteine was followed by NMR using a Bruker DMX NMR spectrometer operating at 500 MHz. All data were acquired on samples equilibrated at 310 K. A triple resonance (TBI−^{1}H, ^{13}C, X) probehead equipped with a single (*z*) axis gradient coil was used for all data accumulation. Calibration and spectrometer setup were carried out using a sample of ^{15}N-**1**, prior to the addition of cysteine.

1D ^{1}H NMR spectra were acquired without ^{15}N-decoupling over a 6 kHz frequency width and acquired with 128 transients into 32K data points (acquisition time = 2.726 s) with a relaxation delay of 1.5 s between transients. ^{1}H pulse calibration was carried out using a presaturation pulse sequence (zgpr). Subsequently, ^{1}H NMR data were either acquired using a DPFGSE routine or its modified form in which composite inversion pulses were applied.[14] In addition, ^{15}N-edited ^{1}H NMR spectra were acquired without ^{15}N-decoupling. This enabled high resolution NMR spectra to be acquired, which could then be compared directly with 1D ^{1}H NMR spectra acquired under the same conditions. In this way, NMR resonances from ^{15}N-attached protons could be directly identified using both gradient-HSQC and gradient-HSQC TOCSY pulse programs. Gradients were used to select for ^{1}H−^{15}N coherences and were simultaneously responsible for eliminating the water resonance.

2D [^{1}H, ^{15}N] HSQC NMR data were acquired, with ^{15}N-decoupling during the acquisition period, over an F2 frequency width of 5 kHz (acquisition time = 204 ms). Multiples of 4 transients were accumulated for each of 256 t_1 increments over an F1 frequency width of 80 ppm centered at −30 ppm relative to $^{15}NH_4Cl$ (reference for 0 ppm). Phase-sensitive data were acquired in a sensitivity-improved manner using an echo−antiecho acquisition mode.[15] 2D [^{1}H, ^{15}N] HSQC TOCSY NMR data were acquired using a similar procedure but incorporating a DIPSI-2 spin-lock of 55 ms duration.

2D [^{1}H, ^{1}H] TOCSY NMR data were acquired over a frequency width of 5 kHz (acquisition time 204 ms) in F2 and F1. A multiple of 16 transients was acquired for each of 512 t_1 increments (TPPI). A spin-lock time of 55 ms and a relaxation delay of 2 s were used. ^{15}N-decoupling was applied using a ^{15}N-refocusing pulse halfway through the incremental delay period together with ^{15}N-GARP-decoupling during t_2.

(c) For the reaction mixtures of complex **1** with L-methionine, ^{1}H NMR and 2D [^{1}H, ^{1}H] TOCSY, NOESY NMR spectra were acquired using a Bruker DMX NMR spectrometer operating at 500 MHz.

All NMR data were processed using Xwin-nmr (version 2.0, Bruker U.K. Ltd.).

pH Measurements. All pH measurements were made using a Corning 240 pH meter equipped with an Aldrich micro combination electrode calibrated with Aldrich standard buffer solutions of pH 4, 7, and 10. NMR samples were prepared in 10% D_2O/90% H_2O. No correction has been applied for the effect of deuterium on the glass electrode.

Preparation of Samples. (a) HPLC. Reaction mixtures of complex **1** with L-cysteine and L-methionine at various molar ratios were prepared by mixing a 10 mM solution of **1** and 50 mM solutions of the amino acids. The mixtures were diluted to the required concentration with deionized water or 50 mM TEAA solution with the relevant pH values and then incubated at 310 K in a water bath for 48 h for the subsequent HPLC analysis.

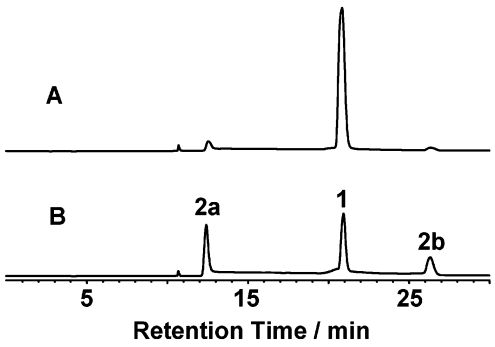

Figure 1. HPLC traces with UV detection at 254 nm for complex **1** (1 mM) in (A) 100 mM NaCl solution, pH 6.92, and (B) water, pH 5.48. Both solutions were incubated for 48 h at 310 K before analysis and were at equilibrium. Peak assignments: **1** [(η^6-biphenyl)RuCl(en)]$^+$; **2a** [(η^6-biphenyl)Ru(H_2O)(en)]$^{2+}$; **2b** [(η^6-biphenyl)Ru(CF_3COO)(en)]$^+$.

The time course of the reaction of complex **1** (1 mM) with L-cysteine (2 mM) at 310 K was followed chromatographically by injection of aliquots of the mixture onto the HPLC column at various time intervals.

The samples for semipreparative separation contained 10 mM of complex **1** and 20 mM of L-cysteine.

(b) ESI-MS. The fractions collected from analytical HPLC separations were frozen in liquid nitrogen, lyophilized using a Modulyo Edwards freeze-drier, and then dissolved in a 50:50 (v/v) mixture of acetonitrile and water for direct infusion. For LC-ESI-MS assays, the samples were prepared by the same method as for the preparation of samples for HPLC separation.

(c) NMR. ^{15}N-**1** (2.776 mg) was dissolved in 0.6 mL of 10% D_2O/90% H_2O, and the 2D [^{1}H,^{15}N] HSQC TOCSY spectrum was recorded after 12 h. Then, 100 μL of 112 mM solution of cysteine in 10% D_2O/90% H_2O was added to the described solution. 2D [^{1}H,^{15}N] HSQC TOCSY or 2D [^{1}H, ^{1}H] TOCSY NMR spectra were recorded at various intervals. For the ^{1}H NMR time course, the reaction mixture contained 6 mM complex **1** and 6 mM L-cysteine. 1D ^{1}H or 2D [^{1}H, ^{1}H] TOCSY and NOESY NMR spectra were recorded for a reaction mixture of complex **1** (5 mM) with L-methionine (5 mM) in 10% D_2O/90% H_2O.

The HPLC-isolated adducts **5** and **6** collected from semipreparative HPLC separations were frozen in liquid nitrogen, lyophilized as described, and then dissolved in 0.6 mL of 10% D_2O/90% H_2O for 1D and 2D ^{1}H NMR spectra.

Results

Hydrolysis of Ruthenium Arene Complex [(η^6-Biphenyl)RuCl(en)][PF_6] (1). First, the hydrolysis of complex **1** in aqueous solution was investigated by HPLC and LC-ESI-MS assays and NMR spectroscopy. This allowed ready identification of any hydrolysis products formed during reactions with amino acids.

HPLC chromatograms for a 1 mM solution of complex **1** in water and in 100 mM NaCl solution are shown in Figure 1. Three species were detected with elution times of 12.25, 20.77, and 26.16 min for an aqueous solution of complex **1**. The subsequent ESI-MS assays showed that the second peak at 20.77 min corresponds to the intact cation of complex **1**, and the first and the third peaks correspond to hydrolysis

(14) Liu, M.; Mao, X.; Ye, C.; Huang, H.; Nicholson, J. K.; Lindon, J. C. *J. Magn. Reson.* **1998**, *132*, 125−129.

(15) (a) Palmer, A. G.; Cavanagh, J.; Wright, P. E.; Rance, M. *J. Magn. Reson.* **1991**, *93*, 151−170. (b) Kay, L. E.; Keifer, P.; Saarinen, T. *J. Am. Chem. Soc.* **1992**, *114*, 10663−10665. (c) Schleucher, J.; Schwendinger, M.; Sattler, M.; Schmidt, P.; Schedletzky, O.; Glaser, S. J.; Sørensen, O. W.; Griesinger, C. *J. Biomol. NMR* **1994**, *4*, 301−306.

product (**2a**) and TFA adduct (**2b**) of **2a**. Detailed mass spectral data are shown in Figure S1.

The 2D [^{1}H,^{15}N] HSQC NMR spectrum (Figure S2) of ^{15}N-**1** (8 mM) in 90% H_2O/10% D_2O incubated at 310 K for 12 h contains two sets of cross-peaks at δ ^{1}H/^{15}N 5.98/−24.5 and 3.93/−24.5 corresponding to intact complex **1** (56%, based on the integrals of cross-peaks), and at δ 6.14/−22.8 and 4.10/−22.8 corresponding to the aqua complex **2a** (44%). The equilibrium constant (*K*) for hydrolysis of complex **1** in aqueous solution is 2.8×10^{-3} M at 298 K, as determined from these NMR data. A detailed kinetic study of the hydrolysis of complex **1** will be published elsewhere.

Reaction of [(η^6-Biphenyl)RuCl(en)][PF_6] with L-Cysteine. UV and HPLC Reaction Course. The UV time course for the reaction of complex **1** (100 μM) with L-cysteine (800 μM) in aqueous solution was followed over a period of 12 h. There were increases in absorbance at 329, 250, and 208 nm, and a decrease in absorbance at 228 nm (Figure S3).

The course of the reaction of complex **1** (1 mM) with L-cysteine (2 mM) in aqueous solution was also followed by HPLC. As shown in Figure 2A, six adducts were separated on a reversed-phase column using an acetonitrile gradient and TFA as ion-pairing agent after a period of 48 h of reaction. The peaks for adducts **4a** and **4b** increased in intensity for 12 h but had disappeared after 48 h, suggesting that they are intermediates. Adducts **5** and **6** appeared after 6 and 24 h, respectively. After 48 h, complex **5** became the dominant product. The peak for adduct **3** increased in intensity slowly up to 24 h of reaction time, and then decreased, but was still detectable after 48 h. Adduct **7a** is a minor product but increased in concentration slowly over the period of 48 h. After 48 h, ca. 50% of complex **1** (based on ICP-AES determination of Ru) had not reacted with L-cysteine; of this, ca. 65% was present as the hydrolysis products (**2a** + **2b**) (Figure 2B). In 100 mM NaCl solution, less of complex **1** (21%) reacted with L-cysteine, and ca. 91% of unreacted complex **1** was present as the chloro complex after 48 h at 310 K. When the reaction was carried out in the absence of air, under N_2, the peak for product **7a** was significantly more intense (Figure 2C).

(LC-)ESI-MS Identification of Adducts. The reaction mixtures of complex **1** (2 mM) with L-cysteine (4 mM) incubated at 310 K for 6 or 48 h were analyzed by LC-ESI-MS. The TIC (total ion count) and UV traces are shown in Figure S4, and the mass spectra of the respective fractions, in Figures 3 and 4, and Figure S5.

In the mass spectrum of the fraction eluting at 11.17 min, singly charged and doubly charged ion peaks were observed at *m*/*z* 554.7 and 277.7 corresponding to a cystine adduct [(η^6-biphenyl)Ru(Cys_2H_2)(en)]$^{2+}$ (**3**) (calcd *m*/*z* 555.1 for [**3** − H]$^+$ and 278.1 for [**3**]$^{2+}$). In addition, a singly charged ion peak at *m*/*z* 240.7 was also detected and is assignable to free cystine (calcd *m*/*z* 241.0 for [Cys_2H_2 + H]$^+$) which results from the fragmentation of adduct **3** (Figure 3A).

The fractions eluting at 13.73 and 15.63 min gave rise to a singly charged ion at *m*/*z* 436.0 corresponding to the quasimolecular ions of cysteine-bound adducts, presumably

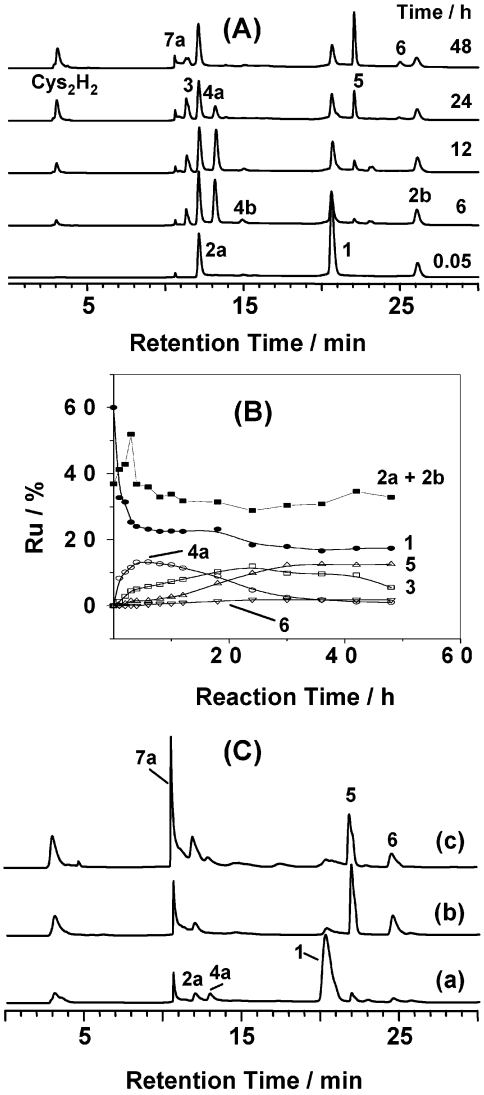

Figure 2. (A) HPLC chromatograms for the reaction of complex **1** (1 mM) with L-cysteine (2 mM) in aqueous solution at 310 K using UV detection at 254 nm over a period of 48 h. (B) Variation in the relative Ru concentrations of various species detected during the described reaction with time. HPLC peaks areas were calibrated by ICP-AES. The relative extinction coefficients for **1**/**2a**/**2b**/**3**/**4a**/**5**/**6** at 254 nm are 1.00/1.15/0.94/1.19/2.11/1.81/2.84. Peaks **4b** and **7a** are minor products and are not plotted. (C) HPLC chromatograms for the reaction of complex **1** (2 mM) with L-cysteine (4 mM) in (a) 100 mM NaCl solution, (b) aqueous solution, and (c) aqueous solution under N_2, at 310 K for 48 h. For peak labels, see Charts 1 and 2. Cys_2H_2 = cystine.

the isomers [(η^6-biphenyl)Ru(*S*-CysH)(en)]$^+$ (**4a**) and [(η^6-biphenyl)Ru(*O*-$CysH_2$)(en)]$^{2+}$ (**4b**) (calcd *m*/*z* 436.1 for [**4a**]$^+$ or [**4b** − H]$^+$) (Figure 3A). It can also be seen that there are two doubly charged ion peaks at *m*/*z* 218.1 and 238.6, assignable to complexes **4a** and **4b** (calcd *m*/*z* 218.5 for [**4a** + H]$^{2+}$ or [**4b**]$^{2+}$), and their adducts with CH_3CN (calcd *m*/*z* 239.0 for [**4a** + CH_3CN +H]$^{2+}$ or [**4b** + CH_3CN]$^{2+}$), a solvent used for HPLC separation. Another singly charged ion was detected at *m*/*z* 314.8 corresponding to the fragment [(η^6-biphenyl)Ru(en)]$^{2+}$ (**F1**, calcd *m*/*z* 315.0 for [**F1** − H]$^+$) resulting from loss of bound cysteine from **4a** or **4b**. It is notable that for adduct **4a** a singly charged ion peak is observed at *m*/*z* 375.8, assignable to the fragment [(η^6-

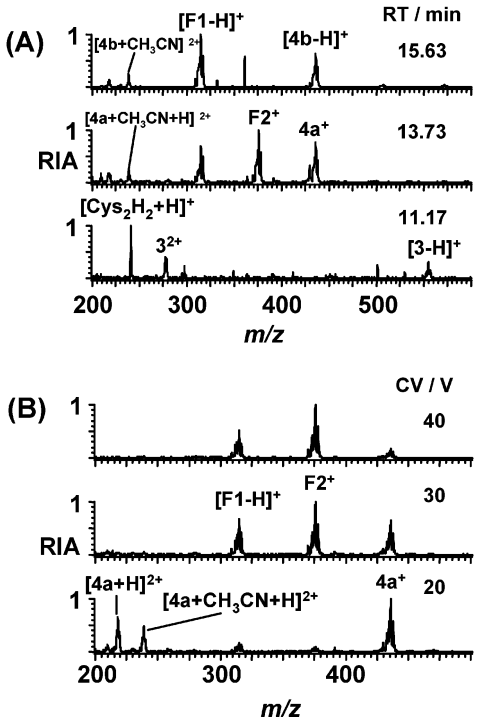

Figure 3. (A) Mass spectra for HPLC fractions with retention times (RTs) of 11.17 (**3**), 13.73 (**4a**), and 15.63 (**4b**) min (see Figure S4) from the reaction mixture of complex **1** (2 mM) with L-cysteine (4 mM) in aqueous solution incubated at 310 K for 6 h. RIA = relative ion abundance. (B) Mass spectra of adduct **4a** at different cone voltages (CVs). At high cone voltages, complex **4a** fragments by loss of cysteine to form fragment $\mathbf{F1}^{2+}$ and by loss of en to form fragment $\mathbf{F2}^{+}$.

biphenyl)Ru(*S*-CysH)]$^+$ (**F2**, calcd *m*/*z* 376.0), formed by loss of bound en from **4a**.

To obtain further structural information, the fractions eluting at 11.17, 13.73, and 15.63 min from the 6 h reaction mixture were also collected by HPLC separation and analyzed by direct infusion ESI-MS at different cone voltages. The results (Figure 3B) confirm that only adduct **4a** eluting at 13.73 min readily gives rise to fragments **F1** at *m*/*z* 314.8 and **F2** at *m*/*z* 375.8 with increase of the cone voltage. With a cone voltage of 40 V, the majority of **4a** is fragmented into **F1** and **F2**. However, no fragment ion **F2** was observed for adducts **3** and **4b** (data not shown), implying that the coordination mode for cysteine in adducts **4a** and **4b** is different.

Figure 4A shows the mass spectra of the fractions eluting at 22.31 and 25.26 min from the 48 h reaction mixture. These show that both adducts are di-ruthenium complexes. In the higher *m*/*z* region, two singly charged ion peaks at *m*/*z* 803.8 and 751.9 are observed, corresponding to the adduct of [(η^6-biphenyl)Ru(H_2O)(μ*S*,*N*-L-Cys)Ru(η^6-biphenyl)(en)]$^{2+}$ (**5**) with TFA (calcd *m*/*z* 804.0 for [**5** − H_2O + TFA]$^+$) and to the quasimolecular ion of [(η^6-biphenyl)Ru(*O*,*N*-L-Cys-*S*)-(*S*-L-Cys-*N*)Ru(η^6-biphenyl)(H_2O)] (**6**) (calcd *m*/*z* 751.0 for [**6** − H_2O + H]$^+$), respectively. Two doubly charged ions of adducts **5** and **6** were detected at *m*/*z* 345.1 (calcd 345.5 for [**5** − H_2O]$^{2+}$) and 376.7 (calcd 376.0 for [**6** − H_2O + 2H]$^{2+}$) with a much greater abundance than those of singly charged ions. In addition, for adduct **5**, there are two lower

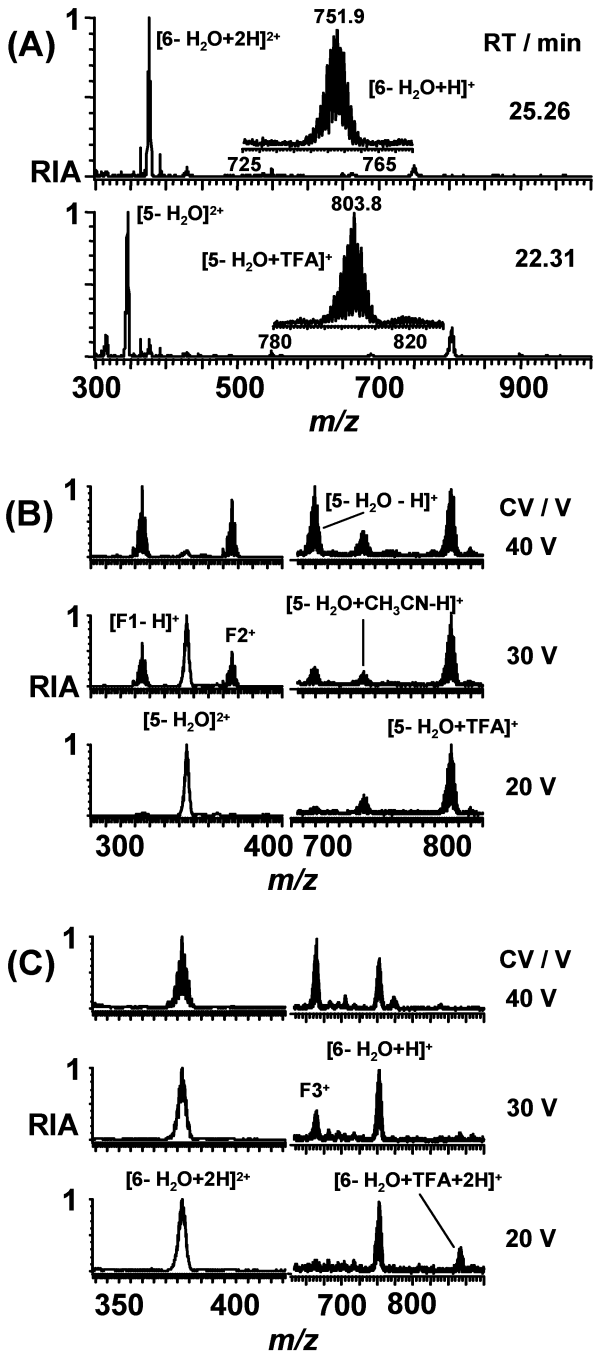

Figure 4. Mass spectra for HPLC fractions from the reaction mixture of complex **1** (2 mM) with L-cysteine (4 mM) in aqueous solution incubated at 310 K for 48 h. For HPLC chromatograms, see Figure S4. (A) Peaks with retention times 22.31 and 25.26 min (adducts **5** and **6**, respectively), (B) variation of cone voltage for adduct **5**, and (C) for adduct **6**. At high cone voltages, the di-ruthenium complex **5** fragments to give mono-ruthenium species $\mathbf{F1}^{2+}$ and $\mathbf{F2}^{+}$; complex **6** fragments by loss of $CH_2(NH_2)CHCOO^-$ from one of the bridging cysteines to give the mono-cysteine-bridged di-ruthenium species $\mathbf{F3}^{+}$. For structures, see Charts 2 and S1.

abundance ion peaks present at lower *m*/*z* values assignable to fragments **F1** and **F2**.

The HPLC-isolated complexes **5** and **6** were also infused directly into the ESI source to study their detailed fragmentation. In the mass spectrum of complex **5** with a cone voltage of 20 V, only one doubly charged ion peak was observed at *m*/*z* 345.1 (Figure 4B). With increase of cone voltage, two

singly charged ion peaks appeared at *m*/*z* 314.8 and 375.8 corresponding to fragments [(η^6-biphenyl)Ru(en)]$^{2+}$ (**F1**) and [(η^6-biphenyl)Ru(*S*-L-CysH)]$^+$ (**F2**). These fragments result from the cleavage of the cysteine bridge between the two ruthenium ions of complex **5**. When the cone voltage was increased to 40 V, the doubly charged ion at *m*/*z* 345.1 almost disappeared, and fragments **F1** and **F2** became dominant. Meanwhile, in the higher *m*/*z* region, at lower cone voltage, two singly charged ion peaks at *m*/*z* 803.8 and 730.8 were detected corresponding to adducts of complex **5** with TFA and CH_3CN (calcd *m*/*z* 731.1 for [**5** − H_2O + CH_3CN − H]$^+$). At a cone voltage of 30 V, a new singly charged ion peak appeared at *m*/*z* 689.9 as expected for the quasimolecular ion of complex **5** (calcd *m*/*z* 690.0 for [**5** − H_2O − H]$^+$) and increased in abundance with increase of cone voltage.

For complex **6** (Figure 4C), only one doubly charged ion peak at *m*/*z* 376.7 was observed in the lower *m*/*z* region even with a high (40 V) cone voltage. In the higher *m*/*z* region, besides the singly charged quasimolecular ion at *m*/*z* 751.9, another singly charged ion peak was detected at *m*/*z* 865.8. This is assigned to the TFA adduct of complex **6** [(η^6-biphenyl)Ru(*O*,*N*-L-Cys-*S*)(*S*-L-Cys-*N*)Ru(η^6-biphenyl)(CF_3-COO)] (calcd *m*/*z* 865.0 for [**6** − H_2O + TFA + 2H]$^+$). Moreover, a new singly charged ion peak at *m*/*z* 664.9 appeared in the higher *m*/*z* region when the cone voltage was increased to 30 V. This new peak corresponds to the fragment ion [(η^6-biphenyl)Ru(SH)(*O*,*N*-L-Cys-*S*)Ru(η^6-biphenyl)]$^+$ (**F3**, calcd *m*/*z* 664.0) resulting from the loss of $CH_2(NH_2)CHCOO^-$ from one of the cysteine bridges between the two ruthenium ions of complex **6**.

Two significant peaks were observed at 2.89 and 10.34 min in the HPLC trace with UV detection for the reaction mixture of complex **1** (2 mM) with L-cysteine (4 mM) (Figure S4A). However, the TIC signals over the range 200−1000 Da (Figure S4B) were not strong enough to allow mass spectra to be recorded for both fractions. Therefore, a larger volume (8 mL) of a more concentrated solution of complex **1** (10 mM) and L-cysteine (20 mM) incubated at 310 K for 48 h was separated by semipreparative HPLC. The fractions eluting at 2.89 and 10.34 min were collected and then directly infused for ESI-MS assays. The mass spectra of the two fractions are shown in Figure S5. For the fraction eluting at 2.89 min, there are two peaks at *m*/*z* 240.7 and 60.8, showing that it contains a mixture of oxidized L-cysteine (calcd *m*/*z* 241.0 for [Cys_2H_2 + H]$^+$) and free ethylenediamine (calcd *m*/*z* 61.1 for [en + H]$^+$). The latter probably results from the loss of en from the S-bound cysteine adduct **4a**.

For the fraction eluting at 10.34 min, two quadruply charged ion peaks were observed (Figure S5B). On the basis of the mass-to-charge ratio and isotopic model, the peak at *m*/*z* 511.8 corresponds to the ruthenium cluster [(biphenyl)-Ru]$_8^{8+}$ (**7a**) (calcd *m*/*z* 510.7 for [**7a** − 4H]$^{4+}$); the second peak at *m*/*z* 592.1 corresponds to an adduct of this cluster with CH_3CN, [(biphenyl)Ru(CH_3CN)]$_8^{8+}$ (**7b**) (calcd *m*/*z* 592.8 for [**7b** − 4H]$^{4+}$). Although these are reasonable assignments, the resolution is not high enough to allow an unambiguous assignment of the overall charge in terms of the oxidation state of Ru (0, +1, or +2) and number of protons gained or lost by the ion.[16]

Table 1. Adduct Ions Detected by LC-ESI-MS Assays of HPLC Fractions from the Reaction of Complex **1** [(η^6- Biphenyl)RuCl(en)]$^+$ with L-Cysteine

RT[a] min	obsd (calcd)[c] *m*/*z*	obsd ions[d]
3.01 (2.89)[b]	60.8 (61.1)	[en + H[e]]$^+$
	240.7 (241.0)	[Cys_2H_2 + H]$^+$
10.85 (10.34)[b]	511.8 (510.7)	[**7a** − 4H[e]]$^{4+}$
	592.1 (592.8)	[**7b** − 4H]$^{4+}$
11.17	277.7 (278.1)	[**3**]$^{2+}$
	554.7 (555.1)	[**3** − H]$^+$
13.73 and	218.1 (218.5)	[**4a** + H]$^{2+}$, [**4b**]$^{2+}$
15.63	238.6 (239.0)	[**4a** + CH_3CN + H]$^{2+}$, [**4b** + CH_3CN]$^{2+}$
	314.8 (315.0)	[F**1** − H]$^+$
	375.8 (376.0)	[F**2**]$^+$
	436.0 (436.1)	[**4a**]$^+$, [**4b** − H]$^+$
22.31	314.8 (315.0)	[F**1** − H]$^+$
	345.1 (345.5)	[**5** − H_2O]$^{2+}$
	375.8 (376.0)	[F**2**]$^+$
	689.9 (690.0)	[**5** − H_2O − H]$^+$
	730.8 (731.1)	[**5** − H_2O + CH_3CN − H]$^+$
	803.8 (804.0)	[**5** − H_2O + TFA]$^+$
25.26	376.7 (376.0)	[**6** − H_2O + 2H]$^{2+}$
	663.9 (664.0)	[F**3**]$^+$
	751.9 (751.0)	[**6** - H_2O + H]$^+$
	865.8 (865.0)	[**6** − H_2O + TFA + 2H]$^+$

[a] RT is the retention time in TIC traces from LC-ESI-MS assays. [b] Retention time for UV detection (see text). [c] Observed (obsd) and calculated (calcd) mass-to-charge ratios for the observed ions. Mass type: monoiso. For mass spectra, see Figures 3, 4, and S5. [d] For structures, see Charts 1, 2, and S1. [e] H indicates gain or loss of a proton.

Table 1 provides a complete list of the ions observed in Figures 3, 4, and S5.

1D ^{1}H and 2D [^{1}H, ^{1}H] NMR Spectra of HPLC-Isolated Di-Ruthenium Complexes 5 and 6. Complexes **5** and **6** were isolated by semipreparative HPLC from a solution (8 mL) of complex **1** (10 mM) and L-cysteine (20 mM) incubated at 310 K for 48 h and were characterized by 1D and 2D ^{1}H NMR spectroscopy. The solutions of **5** and **6** in 10% D_2O/90% H_2O had pH values of 4.0 and 4.2, respectively.

The ^{1}H NMR chemical shift data for complexes **5** and **6** are summarized in Table 2, together with those of complex **1** for comparison. In the ^{1}H NMR spectra of both adducts **5** and **6** (Figure S6), two groups of peaks are present in the aromatic region. The first group is assigned to noncoordinated phenyl rings (Ph1 and Ph3), and the second group, to coordinated rings Ph2 and Ph4 of the biphenyl ligands. For adduct **5**, a single set of cysteine resonances was observed. For adduct **6**, there are two sets of cysteine resonances. Only one set of signals was observed for CH_2 and NH_2 protons of en corresponding to the one en ligand present in adduct **5**. No peaks assignable to en were detected for adduct **6**. This suggests that only one of two Ru ions in **5** has a bound ethylenediamine ligand and that neither Ru has a bound en in adduct **6**. These results agree with those obtained from ESI-MS assays.

(16) Preliminary FTICR-MS studies (Polfer, N.; Wang, F.; Langridge-Smith, P. R. R.; Sadler, P. J. Unpublished.) have allowed detection of the fragment [{biphenyl}Ru)$_4$ + 2H]$^{2+}$ suggesting that at least part of the cluster may contain Ru(0).

Table 2. ^{1}H NMR Chemical Shifts (δ) for Complexes **1**, **4a**, **4b**, **5**, and **6** in 10% D_2O/90% H_2O

		complex (pH)/δ			
proton[a]	**1**[b] (5.5)	**4a** (ca. 3.6)[c]	**4b** (ca. 3.6)[c]	**5**[b] (4.0)	**6**[b] (4.2)
		Phenyl			
H11, H12	7.83 (m)	7.74 (m)	7.92 (m)	7.65 (m)	7.73 (m)
H13, H14, H15	7.64 (m)	7.58 (m)	7.64 (m)	7.64 (m)	7.55 (m)
H21	5.98 (t)	6.09 (t)	6.21 (d)	5.81 (t)	6.21 (d)
H22	5.98 (t)	6.09 (t)	6.21 (d)	5.60 (d)	6.02[d]
H23	6.26 (d)	5.91 (t)	6.08 (t)	6.31 (t)	5.91 (t)
H24	6.26 (d)	5.91 (t)	6.08 (t)	6.17 (t)	6.11 (t)
H25	5.91 (t)	5.75 (d)	5.78 (d)	5.78 (t)	5.76 (t)
H31, H32				7.72 (m)	7.61 (m)
H33, H34, H35				7.68 (m)	7.56 (m)
H41				6.21 (t)	6.16 (d)
H42				6.21 (t)	6.02[d]
H43				5.89 (m)	5.84 (t)
H44				5.89 (m)	6.02[d]
H45				5.78 (t)	5.73 (m)
		en			
NH_2[e]	3.93 (br)	3.54 (m)	4.10 (m)	1.68 (t)	
	5.98 (m)	3.64 (m)	6.07 (m)	3.68 (t)	
		5.47 (m)		5.81 (m)	
CH_2[e]	2.45 (m)	2.45 (m)	2.31 (m)	2.41 (m)	
		2.47 (m)	2.42 (m)	2.31 (m)	
				2.44 (m)	
				2.33 (m)	
		Bound Cys1			
NH_2[e]		*f*	*f*	5.39 (d)	3.64 (t)
		f	*f*	6.31 (t)	7.21 (d)
α-CH		3.83 (t)	3.86 (t)	3.83 (t)	3.70 (t)
β-CH_2[e]		2.94 (dd)	2.85 (dd)	1.99 (d)	2.28 (t)
		3.10 (dd)	2.80 (dd)	2.68 (dd)	2.65 (dd)
		Bound Cys2			
NH_2					5.47 (d)
α-CH					3.58 (t)
β-CH_2					1.86 (t)
					2.31 (dd)

[a] For proton labeling, see Charts 1 and 2. [b] Spectra recorded at 298 K. [c] Spectra recorded during reaction of complex **1** with L-cysteine at 310 K after an average reaction time of 9.8 h. [d] Overlapped with one another. [e] Stereospecific assignment not made. [f] Not observed.

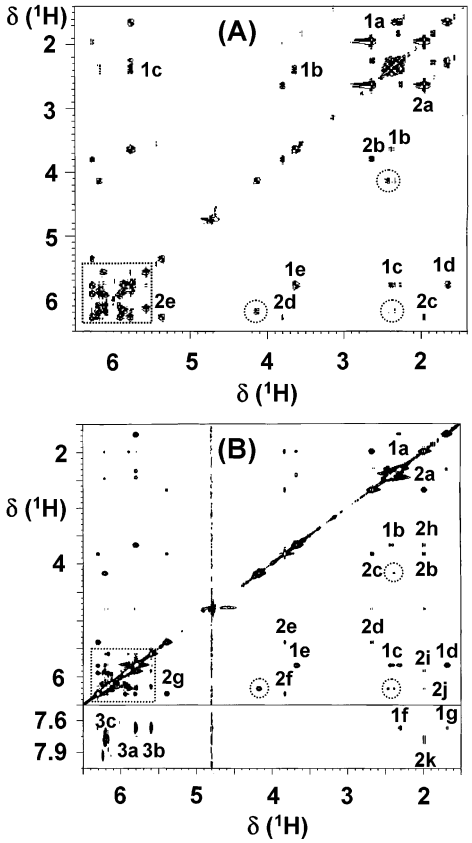

Figure 5. 2D [^{1}H, ^{1}H] NMR spectra of HPLC-isolated complex **5** at 298 K in 90% H_2O/10% D_2O, pH 4.0. (A) COSY spectrum, peak assignments: 1a−c CH_2/NH_2 and 1d−e NH/NH (en), showing that only one bound en is present in this di-ruthenium complex; 2a β-CH/β-CH; 2b β-CH/α-CH; 2c β-CH/α-NH; 2d α-CH/α-NH; and 2e α-NH/α-NH (cysteine). The observation of peak 2c indicates the presence of a five-membered cysteine chelate ring. (B) NOESY spectrum (1 s mixing time). Assignments of NOE cross-peaks: 1a H64 to H67, H68; 1b H62 to H65, H66; 1c H61, H63 to H65, H66, H67, H68; 1d H64 to H63; 1e H62 to H61; 1f H68 to H11, H12, H13, H14, H15; 1g H64 to H11, H12, H13, H14, H15. 2a, H55 to H54; 2b H55 to H53; 2c H54 to H53; 2d H54 to H52; 2e H53 to H52; 2f H53 to H51; 2g H51 to H52; 2h H55 to H62; 2i H55 to H43 and H44; 2j H55 to H41 and H42, 2k H55 to H31 and H32. 3a H21 to H11; 3b H22 to H12; 3c H41, H42 to H31, H32. Notable are cross-peaks 1f,g, which indicate the close proximity of en to Ph1, and 2h−k, which show that H55 of β-CH_2 in cysteine ligand is close to en (H62) and close to Ph3 and Ph4. The NOEs between H61, H63 and H41−H45 are undetectable because of overlapping with the NOEs between the aromatic protons. Dotted squares contain phenyl resonances, and dotted circles, resonances for en of complex **1** (incompletely separated by HPLC). For structure of complex **5** and atom labeling, see Chart 2.

The 2D [^{1}H, ^{1}H] DQF−COSY and NOESY spectra of complex **5** are shown in Figure 5. As shown in the COSY spectrum of **5** (Figure 5A), cross-peaks 1a−e arise from coupling of CH_2 to NH_2 (1a−c) and NH to NH (1d−e) of the bound en. Cross-peaks 2a−e result from coupling of β-CH to β-CH (2a), β-CH to α-CH (2b), α-CH to α-NH (2d), and α-NH to α-NH (2e) of the bound cysteine. It is notable that one cross-peak, 2c (δ 1.99/6.31), is observed corresponding to the coupling of protons H55 (β-CH) to H51 (α-NH), suggesting that there is one conformation of "M" or "W" shape between protons H55 and H51 in a five-membered cysteine chelate ring (Chart 2).

In the 2D [^{1}H, ^{1}H] NOESY NMR spectrum of complex **5** (Figure 5B), two sets of cross-peaks are assignable to NOEs between protons of an en ligand (peaks 1a−e) and between protons of the chelated cysteine bridge (peaks 2a−g). In addition, two cross-peaks at δ 2.31/7.65 (1f) and 1.68/7.65 (1g) due to NOEs between en-H68 (1f), en-H64 (1g), and H11−15 (Ph1) are observed, which indicates the close proximity of the en ring to Ph1. Four cross-peaks at δ 1.99/3.68 (2h), 1.99/5.89 (2i), 1.99/6.21 (2j), and 1.99/7.72 (2k) are assigned to NOEs between H55 and H62 (2h), H43 and H44 (2i), H41 and H42 (2j), and H31 and H32 (2k), respectively, which shows that one proton (H55) of the β-CH_2 in the cysteine chelate ring is close to en-H62 and close to Ph3 and Ph4. Peaks 3a−c are due to NOEs between aromatic protons H21 and H11(3a), H22 and H12 (3b), H41, H42 and H31, H32(3c). The described NMR data, together with 2D [^{1}H, ^{1}H] TOCSY (Figure S7) and ROESY (not shown) spectra support a monochelated, mono-cysteine S-bridged di-ruthenium structure for complex **5**, as shown in Chart 2.

In the 2D [^{1}H, ^{1}H] TOCSY spectrum of complex **6** (Figure 6A), besides the cross-peaks for aromatic protons (in solid boxes), two sets of cross-peaks assignable to two cysteine bridges are observed. Cross-peaks are present for coupling of β-CH to β-CH (1a), β-CH_2 to α-CH (1b,c), β-CH_2 to α-NH_2 (1d−g), α-CH to α-NH_2 (1h,i) and α-NH to α-NH

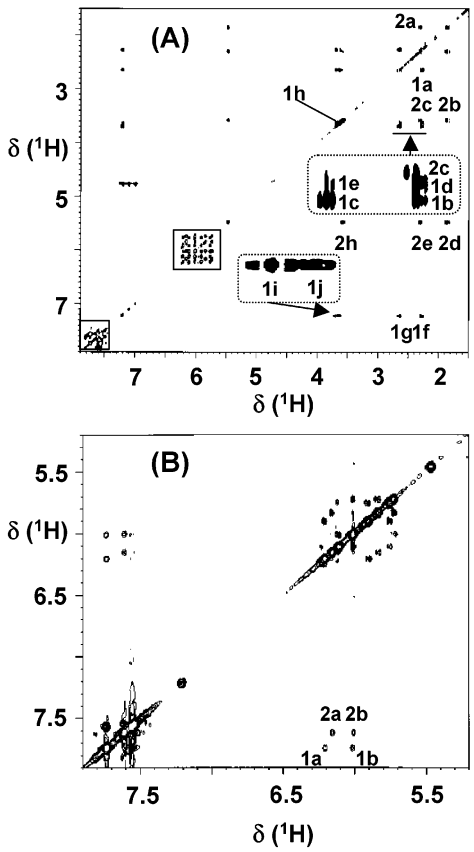

Figure 6. 2D [^{1}H, ^{1}H] NMR spectra of HPLC-isolated complex **6** at 298 K in 90% H_2O/10% D_2O, pH 4.2. The labels shown are for peaks only, for atom labeling system see Chart 2. (A) TOCSY spectrum. Peak assignments: 1a β-CH/β-CH; 1b,c β-CH_2/α-CH; 1d−g β-CH_2/NH_2; 1h,i α-CH/NH_2; 1j NH/NH of Cys1. Peaks 2a β-CH/β-CH; 2b,c β-CH_2/α-CH; 2d,e β-CH_2/NH_2; 2h α-CH/NH_2 of Cys2. Dotted boxes show expansions; solid boxes indicate phenyl resonances. The spectrum shows that two coordinated Cys residues are different: Cys1 is both a chelating and a bridging ligand, whereas Cys2 forms only a bridge between the two Ru ions (i.e., peaks 2f,g,i,j are absent for Cys2). (B) Aromatic region of the NOESY spectrum (1 s mixing time). Assignments of NOE peaks: 1a H11 to H21, 1b H12 to H22, 2a H31 to H41, 2b H32 to H42. The spectrum shows that the diruthenium complex **6** contains two types of coordinated biphenyl ligands and that the protons of bridging Cys ligands are >5 Å away from the biphenyl protons (no NOEs observed).

(1j) of the first cysteine-bridge Cys1, which forms a five-membered *N*,*O*-chelate ring. Another set of cross-peaks (2a−e,h) is due to the second cysteine ligand Cys2 which forms a linear bridge between the two ruthenium ions (Chart 2). No TOCSY cross-peaks assignable to en were observed, again confirming that complex **6** does not contain en. The 2D [^{1}H, ^{1}H] NOESY spectrum (Figure 6B) allowed assignment of peaks for the aromatic systems. Two pairs of cross-peaks, 1a (δ 6.16/7.61) and 1b (δ 6.02/7.61), 2a (δ 6.21/7.73) and 2b (δ 6.02/7.73), are assignable to NOEs between H11 and H21, H12 and H22, H31 and H41, H32 and H42, respectively.

NMR Time Course. The course of the reaction of complex **1** with L-cysteine at 310 K was also followed by 1D ^{1}H NMR (Figure S8A) and 2D [^{1}H, ^{15}N] HSQC TOCSY NMR (Figure 7) spectroscopy using ^{15}N-**1**. The pH of the reaction mixtures decreased from an initial value of 5.12 to 3.53 over a period of 48 h.

After just 15 min of reaction, two triplets at δ 3.86 and 3.83 and two pairs of doublets of doublets were detected, corresponding to the bound cysteines of intermediates **4a** and **4b**. The pair of double doublets at δ 2.85 and 2.80 had almost disappeared after 12 h, and another pair at δ 3.10 and 2.94 disappeared after 24 h. Considering the HPLC time course of this reaction and mass spectra of these adducts, the former pair can be assigned to the β-CH_2 of intermediate **4b**, and the latter, to **4a**. After 6 h, one strong singlet at δ 3.46 appeared and increased in intensity up to 48 h, accompanied by a decrease in intensity of the broad peaks for the en-CH_2 of complex **1**, which implies that this singlet is due to the CH_2 of free ethylenediamine. The ^{1}H NMR spectrum (Figure S8B) and mass spectrum (Figure S5A) of the HPLC fraction eluting at 2.89 min from the reaction mixture of **1** (10 mM) with L-cysteine (20 mM) confirmed that this singlet can be assigned to free ethylenediamine. With the decrease in intensity of peaks for intermediates **4a** and **4b**, a doublet of doublets at δ 2.68 and a doublet at δ 1.99 appeared, corresponding to the β-CH_2 resonances of bound cysteine in adduct **5**. The α-CH peak for bound L-cysteine of **5** was overlapped with that of the intermediate **4a** (δ 3.83). Because of the low percentage (ca. 5% at 48 h, based on the UV absorption) in the reaction mixture, no peaks for adduct **6** were detectable during the ^{1}H NMR time course.

During the course of the reaction as shown in Figure S8A, a triplet (δ 3.99) and a pair of double doublets (δ 3.11, 3.04) due to the α-CH and β-CH_2 of free L-cysteine decreased in intensity and disappeared after 24 h. Meanwhile, a new doublet of doublets at δ 4.12 and a new pair of double doublets at δ 3.21 and 3.40 appeared and can be assigned to the α-CH and β-CH_2 of oxidized L-cysteine. This implies that unbound L-cysteine was completely oxidized to cystine by Ru(II) and/or O_2 from air. During the last stages of the NMR time course, needle-shaped crystals appeared in the NMR tube, attributable to the low solubility of cystine in water.

The course of the reaction of ^{15}N-**1** with L-cysteine as seen by 2D [^{1}H, ^{15}N] HSQC TOCSY NMR is shown in Figure 7, and ^{1}H and ^{15}N chemical shifts are listed in Table 3. The results are consistent with those obtained by HPLC and ^{1}H NMR spectroscopy. During the early period of this reaction (<6 h), three sets of new cross-peaks assignable to adducts **3**, **4a**, and **4b** are present. Cross-peaks 3a, 3b, and 3c are due to the couplings of en-H1/N1 and en-H3/N2 (3a), en-H2/N1 and en-H4/N2 (3b), en-H5, H6/N1 and en-H7, H8/N2 (3c) of complex **3**, and peaks 5a, 5b, and 5c arise from similar couplings for intermediate **4b**. The cross-peaks 4a−d are assigned to en-H1/N1, en-H2/N1, en-H3/N2 and en-H4/N2, and 4g and 4h to en-H5, H6/N1 and en-H7, H8/N2 of intermediate **4a** (atom labeling for en ring is the same as shown in Chart 2 for complex **5**). The presence of cross-peaks 4e (en-H2/N2) and 4f (en-H4/N1) suggests that the two protons en-H2 and en-H4, oriented away from the biphenyl ligand, as well as the two ^{15}N nuclei of the en-NH_2 groups in **4a**, are nonequivalent because of the electronic effect of the sulfur atom and the chirality of the cysteine ligand.

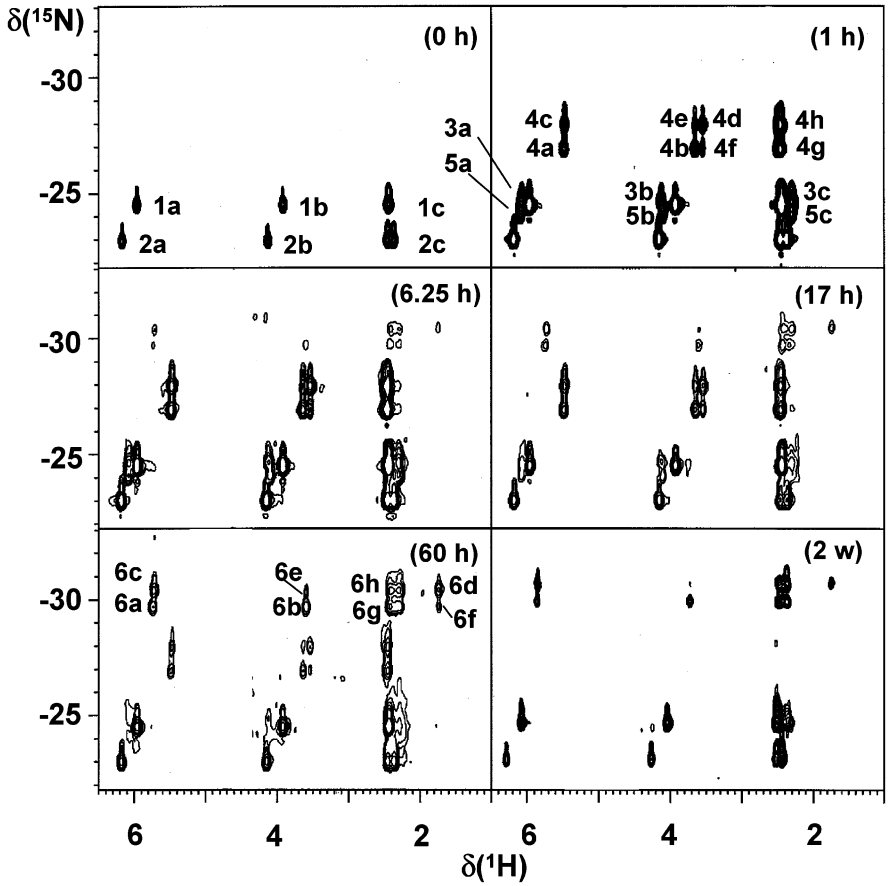

Figure 7. 2D [^{1}H, ^{15}N] HSQC TOCSY NMR time course for the reaction of ^{15}N-**1** (8 mM) with L-cysteine (16 mM) in 90% H_2O/10% D_2O at 310 K over a period of 2 weeks. Assignments: peaks 1a−c from coupling of protons of en-NH_2 (a,b) and protons (c) of en-CH_2 in complex **1** to ^{15}N, 2a−c for complex **2a**, 3a−c for complex **3**, 4a−h for complex **4a**, 5a−c for complex **4b**, 6a−h for complex **5**. For structures, see Charts 1 and 2. Chemical shifts of cross-peaks for adducts **3**, **4a**, **4b**, and **5** are listed in Table 3. It can be seen that complexes **3**, **4a**, and **4b** are intermediates in the reaction. Note that no peaks for complex **6** and free en are observed because complex **6** does not contain bound ^{15}N-en and the NH protons of free protonated en exchange with solvent.

Table 3. Cross-Peaks Observed in the 2D [^{1}H, ^{15}N] HSQC TOCSY Spectra (Figure 7) for Reaction of ^{15}N-**1** with L-Cysteine at 310 K

	δ ^{1}H/^{15}N	
adduct[a]	en-NH_2/en-NH_2	en-CH_2/en-NH_2
3	6.07/−24.7 (3a[b]), 4.12/−24.7 (3b)	2.30/−24.7 (3c)
4a	5.47/−26.9 (4a), 3.64/−26.9 (4b)	2.45/−26.9 (4g)
	5.47/−27.9 (4c), 3.54/−27.9 (4d)	2.45/−27.9 (4h)
	3.64/−27.9 (4e), 3.54/−26.9 (4f)	
4b	6.08/−24.1 (5a), 4.08/−24.1 (5b)	2.30/−24.1 (5c)
5	5.72/−29.6 (6a), 3.60/−29.6 (6b)	2.33, 2.28/−29.6 (6g)
	5.72/−30.4 (6c), 1.74/−30.4 (6d)	2.40, 2.29/−30.4 (6h)
	3.60/−30.4 (6e), 1.74/−29.6 (6f)	

[a] For structures, see Charts 1 and 2. [b] Peak labels used in Figure 7.

After 12 h, a new set of cross-peaks appeared corresponding to the formation of adduct **5**: 6a [en-H1/N1], 6b [en-H2/N1], 6c [en-H3/N2], 6d [en-H4/N2], 6e (en-H2/N2), 6f (en-H4/N1), 6g [en-H5, H6/N1], and 6h [en-H7, H8/N2]. Like those of intermediate **4a**, the two protons en-H2 and en-H4, oriented away from the arene rings Ph3 and Ph4 (Chart 2), and the two ^{15}N nuclei of en-NH_2 groups in complex **5**, are nonequivalent, leading to the presence of cross-peaks 6e and 6f. Over the reaction course, no signal appeared in the 2D [^{1}H, ^{15}N] HSQC NMR spectra corresponding to the formation of **6**, which therefore does not have a bound ^{15}N-en ligand. The cross-peaks 1a−c and 2a−c are due to intact complex **1** and its hydrolysis product **2a** (also see Figure S2).

Figure 8 shows a 2D [^{1}H, ^{1}H] TOCSY NMR spectrum for the reaction of ^{15}N-**1** (8 mM) with L-cysteine (16 mM) at 310 K after an average reaction time of 9.8 h. It can be seen that there is one set of cross-peaks assignable to the coupling of CH_2/NH_2 (1a,b), NH/NH (1c,d) of an en ligand, and α-CH/β-CH_2 (1e) of an L-cysteine ligand for intermediate **4a**. Another set of cross-peaks can be assigned to intermediate **4b**: 2a and 2b to en-CH_2/en-NH_2, 2c to en-NH/en-NH, and 2d to α-CH/β-CH_2 of the L-cysteine ligand. No cross-peaks were observed for the protons of the α-amino groups NH_2 of **4a** and **4b**. However, a group of cross-peaks (inside the dotted box of Figure 8) is assignable to correlation of the water protons with α-CH and β-CH_2 of **4a** and **4b**. This suggests that the α-NH_2 groups of **4a** and **4b** are protonated. The NH_3^+ protons of the cysteine residue correlate with α-CH and β-CH_2 protons via TOCSY as expected, but during the TOCSY mixing time, NH_3^+ protons exchange with H_2O protons, and the NH_3^+ protons carry the correlation effect with them as they change their identity between NH_3^+ and H_2O. Hence, these cross-peaks were observed at the H_2O resonance position. The ^{1}H chemical shifts of intermediates **4a** and **4b** are also listed in Table 2.

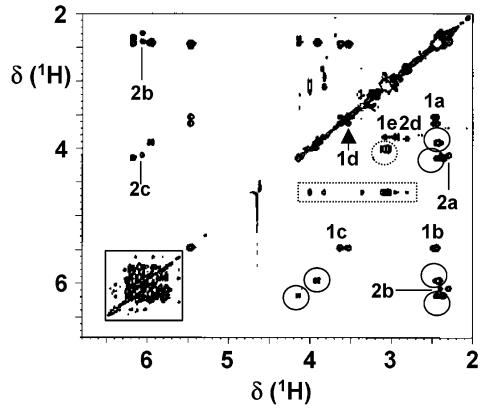

Figure 8. 2D [^{1}H, ^{1}H] TOCSY NMR spectrum for the reaction of complex **1** with L-cysteine (8:16 mM) at 310 K after an average reaction time of 9.8 h. This spectrum allows characterization of the reaction intermediates **4a** and **4b** which cannot be obtained in sufficient quantities by HPLC separation. Assignments: peaks 1a,b en-CH_2/en-NH_2, 1c,d en-NH/en-NH, 1e α-CH/β-CH_2 for complex **4a**. Peaks 2a,b, en-CH_2/en-NH_2, 2c en-NH/en-NH, 2d α-CH/β-CH_2 for complex **4b**. The solid circles contain resonances for complexes **1** and **2a**, the dotted circle, resonances for α-CH/β-CH_2 of free cysteine, and the solid square, resonances for phenyl protons. The dotted box contains cross-peaks assignable to the correlation of NH_3^+ protons to α-CH of free cysteine and **4a**; CH_2 of free en; β-CH_2 of free cysteine, **4a** and **4b** (from left to right).

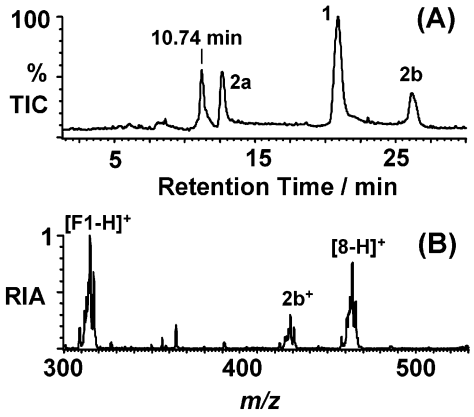

Figure 9. (A) HPLC trace (detected by total ion count, TIC) for the reaction of complex **1** (2 mM) with L-methionine (4 mM) at 310 K after 48 h. (B) Mass spectrum of the HPLC fraction eluting at 10.74 min. This allows the identification of complex **8** as a 1:1 adduct (see Chart 3). For other peak labels, see Charts 1 and S1.

Neither in the 1D ^{1}H NMR time course (Figure S8A) of the reaction of complex **1** with L-cysteine nor in the 2D [^{1}H, ^{1}H] TOCSY NMR spectrum (Figure 8) of this reaction mixture after an average reaction time of 9.8 h at 310 K are there peaks assignable to α-CH, β-CH_2, and α-amino group of adduct **3**. One possible explanation is that the NMR signals of O-bound cystine in **3** are overlapped with those of free cystine or the intermediate **4b**.

Dependence on pH and Molar Ratio. Further studies indicated that the pathway of the reaction of complex **1** with L-cysteine strongly depends on pH and the molar ratio of complex **1** to L-cysteine. The HPLC traces (Figure S9A) for reaction mixtures in 50 mM triethylammonium acetate (TEAA) solutions at different pH values show that the final dinuclear adducts **5** and **6** are detected only when pH is lower than 5. Above this pH, the hydrolysis product of complex **1** becomes dominant. The aqua ligand in **2a** is partly replaced by acetate, and subsequently by TFA on the HPLC column to form **2b**, leading to an increase in intensity of the HPLC peak for **2b**. The acetate adduct of complex **2a** appears to be less reactive toward the thiol. However, the O-bound adduct **4b** increases in intensity with increase of pH (Figure S9A). When the pH of the reaction mixture was higher than 7, more L-cysteine was oxidized to cystine, and less bound to ruthenium.

At higher molar ratios of L-cysteine/**1** and at lower pH, more complex **1** reacted with cysteine, but the proportion of dinuclear adduct **5** decreased and that of **6** increased as shown in Figure S9B. In this case, after 48 h, significant peaks were still detectable corresponding to the intermediate **4b**. On the other hand, with a higher excess of L-cysteine, larger amounts of ruthenium cluster **7a** formed, and **7a** was the dominant product instead of **5**. Aqueous solutions of **7a** were green with two absorption bands at 393.7 and 588.2 nm (Figure S10). Further studies on this unusual ruthenium cluster are being carried out.

Reaction of [(η^6-Biphenyl)RuCl(en)][PF_6] with L-Methionine. An aqueous solution containing 2 mM complex **1** and 4 mM L-methionine was incubated at 310 K for 48 h, during which time the pH decreased from 6.64 to 3.75. The HPLC chromatogram for this reaction mixture detected by total ion counts (TIC) (Figure 9A) shows only one new peak at 10.74 min. One singly charged ion peak at *m*/*z* 463.8 was observed in the subsequent LC-ESI-MS assay for this fraction (Figure 9B), indicating that this adduct, [(η^6-biphenyl)Ru(*S*-L-MetH)(en)]$^{2+}$ (**8**), contains one methionine ligand which has displaced the Cl ligand from complex **1** (calcd *m*/*z* 464.1 for [**8** − H]$^+$). This reaction was also slow, with a $t_{1/2}$ of 2.3 h on the basis of the HPLC time course shown in Figure S11. On the basis of the UV absorption at 254 nm, ca. 73% of original ruthenium complex had not reacted with methionine after 48 h.

The 2D [^{1}H, ^{1}H] TOCSY NMR spectrum at 298 K of a solution containing complex **1** and L-methionine (5:5 mM, final pH 3.64) which had reacted at 310 K for 48 h shows three new cross-peaks at δ 6.24/6.34, 6.00/6.34, and 6.00/6.24 assignable to coupling of the aromatic protons (Ph2) of adduct **8** (Figure 10). Another set of cross-peaks a−c can be reasonably assigned to coupling of en-CH_2/en-NH_2 (a, b) and en-NH/en-NH (c) of **8**. In the region expected for α-CH, β-CH_2, γ-CH_2, and CH_3 of methionine, a set of new cross-peaks (d−h) appeared, corresponding to the connectivities of β-CH_2 to α-CH (d), γ-CH_2 to α-CH (e), β-CH to β-CH (f), and γ-CH_2 to β-CH_2 (g, h) of the bound methionine of **8**. No signals assignable to the α-NH_2 of bound methionine were observed, suggesting that this amino acid functional group remains protonated and is not involved in coordination.

In the 2D [^{1}H, ^{1}H] NOESY spectrum of the same solution (data not shown), only one new cross-peak at δ 6.34/7.69 was observed and is assigned to an NOE between H11, H12 and H21, H22 of Ph1 and Ph2 in adduct **8** (for the structure, see Chart 3). Table 4 shows a complete list of ^{1}H chemical shifts of the L-methionine complex **8** and free L-methionine, together with the coordination shifts of L-methionine. As

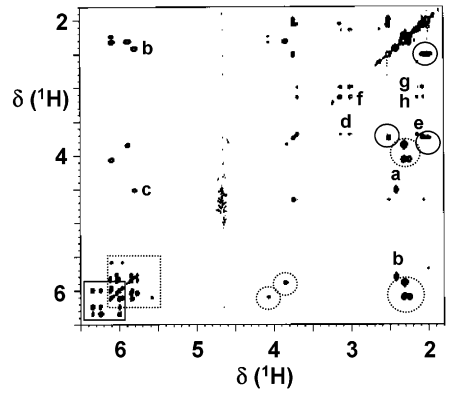

Figure 10. 2D [^{1}H, ^{1}H] NMR TOCSY spectrum for the reaction mixture of complex **1** (5 mM) with L-methionine (5 mM) in 90% H_2O/10% D_2O incubated at 310 K for 48 h, final pH 3.64. Peak assignments: a, b en-CH_2/en-NH_2, c en-NH/en-NH, d γ-CH_2/α-CH, e β-CH_2/α-CH, f γ-CH/γ-CH, g, h β-CH_2/γ-CH_2 for bound methionine. Solid squares contains phenyl resonances of adduct **8**, the dotted square contains those of complexes **1** and **2a**, dotted circles contain resonances for the en of complexes **1** and **2a**, and solid circles contain resonances for unbound L-methionine.

Table 4. ^{1}H NMR Chemical Shifts (δ) of Adduct **8** from the Reaction of Complex **1** with L-Methionine and Free L-Methionine in 10% D_2O/90% H_2O (pH 3.64)

	complex/δ		
proton[a]	**8**[b]	L-Met	$\Delta\delta$[c]
	Phenyl		
H11, H12	7.69 (m)		
H13, H14, H15	7.51 (m)		
H21, H22	6.34 (t)		
H23, H24	6.24 (t)		
H25	6.00 (t)		
	en		
NH_2[d]	4.52 (br)		
	5.80 (br)		
CH_2	2.43 (br)		
	L-Met		
NH_2	*e*	*e*	
α-CH	3.69 (t)	3.73 (t)	−0.04
β-CH_2[d]	2.06 (m)	2.00 (m)	0.06
	2.16 (m)	2.06 (m)	0.10
γ-CH_2[d]	3.01 (m)	2.51 (t)	0.50
	3.14 (m)	2.51 (t)	0.63
CH_3	2.53 (s)	2.01 (s)	0.52

[a] For atom labeling, see Chart 3. [b] Spectrum recorded for the reaction mixture, **1**/Met = 5/5 mM, 310 K, after 48 h. [c] $\Delta\delta = \delta$ (**8**) − δ (L-Met) = coordination shift. [d] Stereospecific assignments not made. [e] Not observed.

shown in Table 4, the protons of the γ-CH_2 and CH_3 of bound L-methionine give rise to larger coordination shifts than those of the α-CH and β-CH_2, suggesting that adduct **8** is the S-bound L-methionine ruthenium complex [(η^6-biphenyl)Ru(*S*-L-MetH)(en)]$^{2+}$.

Discussion

Although the cobalt corrin vitamin B_{12} (deoxyadenosylcobalamine) is a naturally occurring organometallic compound, the wider potential medical applications of organometallic chemistry have only recently attracted attention. The cyclopentadienyl complex Cp_2TiCl_2 has been in clinical trials[17] as an anticancer agent although the results have not been encouraging,[18] and a range of related cyclopendadienyl complexes, including those of V, Nb, Fe, Mo, Ge, and Sn, are also active.[19] Specific targeting of Fe cyclopentadienyl complexes can be achieved by incorporating substituents onto the cyclopentadienyl rings which are recognized by cellular receptors. The complex ferrocifen 1-[4-(2-dimethylaminoethoxy)]-1-(phenyl-2-ferrocenyl-but-1-ene),[20] for example, is a candidate for clinical trials against breast cancer.

Organometallic ruthenium complexes have been reported to exhibit antitumor activity,[3,4,6] but most interest in the biological activity of ruthenium compounds has centered on Ru(III) complexes.[7,8,10c] In view of the usual kinetic inertness of Ru(III), these complexes are thought to be activated in vivo by reduction to Ru(II).[21] Ru(II) complexes can be stabilized by arene ligands, and we have found recently[3] that arene Ru(II) complexes containing a chelated ethylenediamine ligand and additional monodentate ligand exhibit anticancer activity, an example being [(η^6-biphenyl)Ru(en)(Cl)][PF_6], complex **1**.[4] To elucidate the mechanism of action of complex **1**, it is important to investigate potential reactions with biomolecules. Here, we have studied reactions with sulfur-containing amino acids L-cysteine and L-methionine, which are known to play important roles in the metabolic chemistry of platinum anticancer drugs.[22] In general, the biological chemistry of ruthenium arene complexes is relatively unexplored, although there have been several reports of the isolation of amino acid and peptide adducts and their use as synthetic reagents[23,24] or as chiral catalysts.[25,26]

Pathways for Reactions of [(η^6-Biphenyl)Ru(en)Cl]$^{2+}$ with L-Cysteine and L-Methionine. The HPLC and NMR time courses and ESI-MS and NMR data for the adducts allow a reaction course to be drawn up for L-cysteine as

(17) (a) Köpf-Maier, P. *Prog. Clin. Biochem. Med.* **1989**, *10*, 151−184. (b) Köpf-Maier, P.; Neuse, E.; Klapotke, T.; Köpf, H. *Cancer Chemoth. Pharmacol.* **1989**, *24* (1), 23−27. (c) Christodoulou, C. V.; Ferry, D. R.; Fyfe, D. W.; Young, A.; Doran, J.; Sheehan, T. M. T.; Eliopoulos, A.; Hale, K.; Baumgart, J.; Saas, G.; Keer, D. J. *J. Clin. Oncol.* **1998**, *16*, 2761−2769.

(18) (a) Mross, K.; Robben-Bathe, P.; Edler, L.; Baumgart, J.; Berdel, W. E.; Fiebig, H.; Unger, C. *Onkologie* **2000**, *23*, 576−579. (b) Krodger, N.; Kleeberg, U. R.; Mross, K.; Edler, L.; Sass, G.; Hossfeld, D. K. *Onkologie* **2000**, *23*, 60−62.

(19) (a) Köpf, H.; Köpf-Maier, P. *Angew. Chem., Int. Ed. Engl.* **1979**, *18*, 477−478. (b) Köpf-Maier, P.; Köpf, H. In *Metal Compounds in Cancer Therapy*; Fricker, S. P., Ed.; Chapman & Hall: London, 1994; pp 109−146.

(20) Top, S.; Dauer, B.; Vaissermann, J.; Jaouen, G. *J. Organomet. Chem.* **1997**, *541*, 355−361.

(21) (a) Clarke, M. J. *Met. Ions Biol. Syst.* **1980**, *11*, 231−283. (b) Laliberte, J. F.; Sun, I. L.; Crane, F. L.; Clarke, M. J. *J. Bioenerg. Biomembr.* **1987**, *19*, 69−81. (c) Stanbury, D. M.; Hass, O.; Taube, H. *Inorg. Chem.* **1980**, *19*, 518−524.

(22) (a) Reedijk, J.; Teuben, J. M. In *Cisplatin Chemistry and Biochemistry of a Leading Anticancer Drug*; Lippert, B., Ed.; Wiley-VCH: Germany, 1999; pp 339−362. (b) Barnham, K. J.; Djuran, M. I.; Murdoch, P. del S.; Ranford J. D.; Sadler, P. J. *Inorg. Chem.* **1996**, *35*, 1065−1072.

(23) Severin, K.; Bergs, R.; Beck, W. *Angew. Chem., Int. Ed. Engl.* **1998**, *37*, 1634−1654.

(24) (a) Haas, K.; Beck, W. *Eur. J. Inorg. Chem.* **2001**, 2485−2488. (b) Hoffmüller, W.; Maurus, M.; Severin, K.; Beck, W. *Eur. J. Inorg. Chem.* **1998**, 729−731. (c) Severin, K.; Mihan, S.; Beck, W. *Chem. Ber.* **1995**, *128*, 1117−1125.

(25) Davenport, A. J.; Davies, D. L.; Fawcett, J.; Garratt, S. A.; Russell, D. R. *J. Chem. Soc., Dalton Trans.* **2000**, 4432−4441.

(26) (a) Davies, D. L.; Fawcett, J.; Graratt, S. A.; Russell, D. R. *Organometallics* **2001**, *20*, 3029−3034. (b) Carmona, D.; Vega, C.; Lahoz, F. J.; Atencio, R.; Ore, L. A.; Lamata, P. M.; Viguri, F.; San Jose, E. *Organometallics* **2000**, *19*, 2273−2280.

Scheme 1

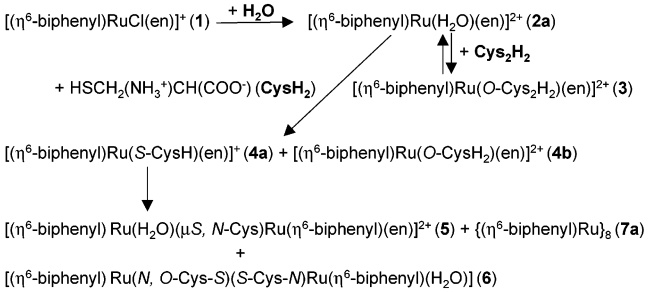

shown in Scheme 1. In aqueous solution (at 310 K, pH 5.12), L-cysteine reacts with the hydrolysis product (**2a**) of complex **1** to give S-bound and O-bound intermediates [(η^6-biphenyl)Ru(*S*-CysH)(en)]$^+$ (**4a**) and [(η^6-biphenyl)Ru(*O*-CysH$_2$)(en)]$^{2+}$ (**4b**). Meanwhile, cysteine is partly oxidized to cystine, which may involve O_2 and/or Ru(II) as the oxidant. Cystine slowly displaces the aqua ligand of **2a** to form the O-bound cystine adduct [(η^6-biphenyl)Ru(*O*-Cys$_2$H$_2$)(en)]$^{2+}$ (**3**). Because of the electronic effect of sulfur, the S-bound intermediate **4a** is slowly converted into the di-ruthenium adducts [(η^6-biphenyl)Ru(H$_2$O)(μ*S*,*N*-L-Cys)Ru(η^6-biphenyl)(en)]$^{2+}$ (**5**) and [(η^6-biphenyl)Ru(*O*,*N*-L-Cys-*S*)(*S*-L-Cys-*N*)Ru(η^6-biphenyl)(H$_2$O)] (**6**) via chelate ring-opening and displacement of en by cysteine.

An indication that L-cysteine can reduce Ru(II) to Ru(I), or even Ru(0), is given by the formation of the unusual ruthenium cluster species {(biphenyl)Ru}$_8$ (**7a**). The amount of this species increased sharply at high concentrations of L-cysteine (Figure S9B). The resolution of the mass spectral peaks was too low to allow unambiguous identification of both the oxidation state of Ru and the number of bound protons. Further high resolution mass spectral studies will be needed to fully characterize this new cluster.[16] Ru(II), Ru(I), and Ru(0) states of diruthenium polycyclic arene complexes are known,[27] but no electrochemical data are available yet for Ru(II) arene diamine complexes. Small arene Ru(I)-containing clusters have been reported previously. The Ru$_8$ cluster [(η^6-C$_6$H$_6$)$_2$(η^6-C$_6$Me$_6$)$_4$Ru$_8$(μ_2-H)$_2$(μ_3-O)$_2$(μ_2-Cl)$_2$]$^{2+}$ has recently been reported by Faure et al.[28] and consists of two tetrahedral Ru$_4$ substructures bridged by a Ru(μ_2-Cl)$_2$Ru linkage. Each substructure appears to contain three Ru(I) arene units. Our cluster may therefore be an elaboration of this substructure. We are carrying out further work to investigate this.

The course of the reaction of complex **1** with L-cysteine depends strongly on pH. In 50 mM TEAA solutions, when the pH was higher than the pK_a of acetic acid (4.75), the reaction was suppressed because of the formation of the less reactive acetate adduct. However, the carboxylate-bound cysteine adduct **4b** predominates (Figure S9A). When the pH value was lower than 5, the dinuclear adducts **5** and **6** were the dominant products, but ca. 50% of the original ruthenium arene complex remained unreacted, of which ca. 47% was present as the aquated product (**2a**). Although **2a** appears to be reactive toward the thiol, oxidation of cysteine accounts for the lack of further reaction.

The reaction of complex **1** with L-methionine was slow with a $t_{1/2}$ of 2.3 h and relatively simple, with only one monodentate adduct [(η^6-biphenyl)Ru(*S*-MetH)(en)]$^{2+}$ (**8**) as product. For the reaction of 2 mM complex **1** with 4 mM L-methionine in aqueous solution at 310 K, after 48 h, 73% of the original ruthenium arene complex remained unreacted, of which ca. 44% was present as the aquated product. This implies that (arene)Ru(II)−S(thioether) bonds are relatively weak.

In the cyclopentadienyl complex [(η^5-C$_5$Me$_5$)Ru(L-Met)],[29] methionine has been reported to be tridentate forming five- and six-membered chelate rings. Other examples of bis-(chelate) complexes with five- and six- or seven-membered rings are the half-sandwich Ru(II) arene complexes with L-methionyglycinate[30] and β-, γ-amino acid esters.[24a] The ethylenediamine ligand in complex **1** prevents methionine chelation.

Structures of Mono-Ruthenium Cysteine Adducts. The ESI-MS fragmentation of adduct **4a** (Figure 3B) and formation of dinuclear adducts **5** and **6** suggests that en labilization and ring-opening take place both during the electrospray ionization and during the reaction of complex **1** with L-cysteine. The presence of a Ru−S bond in intermediate **4a** may account for the labilization. Both sulfur and carbon ligands are known to exhibit high trans effects in Pt(II) chemistry.[22b,31] For example, reactions of [Pt(en)(H$_2$O)$_2$]$^{2+}$ with L-cysteine-derivatives are accompanied by en ring-opening.[32]

The α-NH$_2$ groups of intermediates **4a** and **4b** exchange their protons rapidly with water protons, implying that the α-NH$_2$ groups of **4a** and **4b** are protonated and not coordinated to Ru. Furthermore, the fragmentation of **4a** and **4b** in ESI-MS assays (Figure 3) suggested that **4b** has a different coordination mode compared to **4a** and, thus, is an O-bound cysteine adduct. The ^{15}N chemical shifts of en-NH$_2$ of adduct **3** are close to those of **4b** (Figure 7), suggesting that they both contain an O-bound ligand and that **3** is the O-bound cystine adduct [(η^6-biphenyl)Ru(*O*-Cys$_2$H$_2$)(en)]$^{2+}$. Both HPLC and NMR time courses indicate that adduct **3** slowly reverts to complex **2a** via substitution of cystine by water and disappears after 2 weeks (Figure 7).

Structures of Di-Ruthenium Cysteine Adducts. The 2D [^{1}H, ^{1}H] NMR COSY and NOESY spectra (Figures 5 and 6) of adducts **5** and **6**, as well as the fragmentation in ESI-MS (Figure 4), unambiguously show that they are di-ruthenium complexes. Complex **5** contains two biphenyl, one

(27) Plitzko, K.-D.; Boekelheide, V. *Angew. Chem., Int. Ed.* **1987**, *26*, 700−702.
(28) Faure, M.; Stœckli-Evans, H.; Süss-Fink, G. *Inorg. Chem. Commun.* **2002**, *5*, 9−11.
(29) Sheldrick, W. S.; Gleichmann, A. *J. Organomet. Chem.* **1994**, *470*, 183−187.
(30) Prem, M.; Polborn, K.; Beck, W. *Z. Naturforsch.* **1998**, *53b*, 1501−1505.
(31) (a) Prinsloo, F. F.; Pienaar, J. J.; van Eldik, R. *J. Chem. Soc., Dalton Trans.* **1995**, 3581−3589. (b) Schmülling, M.; Ryabov, A. D.; van Eldik, R. *J. Chem. Soc., Dalton Trans.* **1994**, 1257−1263. (c) Schmülling, M.; Grove, D. M.; van Koten, G.; van Eldik, R.; Veldman, N.; Spek, A. L. *Organometallics* **1996**, *15*, 1384−1391.
(32) Rau, T.; Alsfasser, R.; Zahl, A.; van Eldik, R. *Inorg. Chem.* **1998**, *37*, 4223−4230.

en, and one cysteine ligands, and **6**, two biphenyl and two cysteine ligands. The chemical shift of the α-NH_2 group suggests that the cysteine ligand of **5** forms a five-membered S/N chelate ring and that **6** contains a five-membered N/O chelate ring. The second cysteine ligand in complex **6**, from which the $CH_2NH_2CHCOO^-$ group is readily lost during ESI-MS assays (Figure 4C) and for which the α-NH_2 ^{1}H resonances are equivalent, appears to adopt a bridging conformation (Chart 2). Therefore, **5** is a di-ruthenium complex containing two half-sandwich units linked by a mono-chelated S-bridged cysteine, whereas the two half-sandwich units of **6** are linked by one monochelated bridging cysteine and a second bridging cysteine. One di-ruthenium amino acid complex [(η^6-C_6H_6)Ru(*l*-pen)Cl_2]$_2Cl_2$ has been reported previously.[33] However, the penicillamine ligands in this complex form two five-membered N,S chelate rings, and the two thiolate sulfur atoms form bridges between the two ruthenium atoms to give a four-membered RuSRuS-ring. Because such a ring does not appear to be present in complexes **5** and **6**, the en ligand in **1** plays an important role in determining the nature of the dinuclear products formed here.

Models of complexes **5** and **6** (Figure S12) were constructed using data from the X-ray crystal structure of complex **1**[5] and the di-ruthenium *l*-penicillamine complex.[33] Because of the presence of the S-bridge and two chelate rings (en ring and chelate cysteine), only one model could be built for **5** [*R*(Ru1)*R*(α-C1)], whereas, it was possible to build four isomers for complex **6**: *R*(Ru1)*R*(α-C1)*R*(Ru2)*S*(α-C2), *R*(Ru1)*R*(α-C1)*R*(Ru2)*R*(α-C2), *S*(Ru1)*R*(α-C1)*R*(Ru2)*R*(α-C2), and *S*(Ru1)*R*(α-C1)*R*(Ru2)*S*(α-C2). The model for **5** also confirms the proximity of the en ring to Ph1 and the proximity of the cysteine chelate ring to Ph3 and Ph4 (Figure 5B). Only one set of 1D and 2D ^{1}H NMR peaks was detected for **6** in acidic solution, suggesting that the presence of solvent stabilizes one of the four possible configurations or that there is rapid interconversion on the NMR time scale.

Applications of HPLC and ESI-MS. The ionic nature of adducts of metallodrugs with amino acids and peptides has led to an emphasis on reversed-phase liquid chromatography, often with the use of ion-pairing reagents (IPRs), for the separation of products from reactions in aqueous solutions.[34] Because of its volatility, trifluoroacetic acid (TFA) was used as an ion-pairing reagent (IPR) in the present study. The results show that with 0.1% of TFA present and a suitable acetonitrile gradient, adducts of complex **1** with water, L-cysteine, or L-methionine in aqueous solution can readily be separated. However, the subsequent ESI-MS assays indicate that the hydrolysis product **2a** partly forms a TFA adduct [(η^6-biphenyl)Ru(CF_3COO)(en)]$^+$ **2b** on the HPLC column and during the electrospray ionization (Figures 1 and S1) via displacement of H_2O by trifluoracetate. Also, the di-ruthenium adducts **5** and **6** give rise to TFA adducts during ESI-MS analysis (Figure 4). Fortunately, the TFA adducts present no significant interference in ESI-MS identification of these adducts. In contrast, the formation of TFA adducts suggests the presence of an aqua ligand in complexes **2a**, **5**, and **6**. ESI-MS has become a powerful technique for the characterization of organometallic compounds and their adducts with biological molecules,[35] in particular, when used in combination with HPLC separations.[36] In this work, HPLC-ESI-MS assays allowed not only identification of amino acid adducts of complex **1** but also determination of the specific metal binding sites by fragmentation patterns.

Conclusions and Biological Implications

The anticancer ruthenium arene complex [(η^6-biphenyl)RuCl(en)]$^+$ (**1**) reacts slowly with L-cysteine in aqueous solution at 310 K, initially giving rise to three mononuclear adducts and then, after 24 h, two di-ruthenium adducts. The two di-ruthenium complexes [(η^6-biphenyl)Ru(H_2O)(μ*S*,*N*-L-Cys)Ru(η^6-biphenyl)(en)]$^{2+}$ (**5**) and [(η^6-biphenyl)Ru(*O*,*N*-L-Cys-*S*)(*S*-L-Cys-*N*)Ru(η^6-biphenyl)(H_2O)] (**6**), isolated by HPLC and characterized by LC-ESI-MS and NMR spectroscopy, are the first examples of di-ruthenium arene amino acid complexes containing bridging cysteine. Also, complex **1** is not highly reactive toward the thioether methionine under the conditions used here. The presence of the en ligand has a significant effect on the biological chemistry of the ruthenium arene complex **1**.

In the presence of a large molar excess of cysteine, complex **1** reacted to give significant amounts of an apparent Ru_8 cluster. Because biological cells usually contain millimolar amounts of the tripeptide glutathione (γ-Glu−Cys−Gly), such cluster formation could be of significance inside cells. This is being further investigated.

The slowness of the reactions of complex **1** with these sulfur-containing amino acids and also with L-histidine (unpublished data), and high reactivity toward the DNA base guanine,[5] suggests that adducts with DNA may form even in the presence of amino acids, peptides, and proteins. In contrast, Ru(III) anticancer complexes are thought to bind more strongly to proteins than to DNA. For example, *trans*-indazolium(bisindazole) tetrachloro-ruthenate(III) (**Ru-In**), *trans*-imidazolium (bisimidazole) tetrachloro-ruthenate(III) (**Ru-Im**), and Na[*trans*-$RuCl_4(Me_2SO)$(Im)] [**NAMI**] form strong complexes with the plasma proteins albumin and transferrin, and the latter protein may be responsible for the delivery of Ru(III) to cancer cells.[37] We find that (arene)-

(33) Sheldrick, W. S.; Heeb, S. *J. Organomet. Chem.* **1989**, *377*, 357−366.
(34) (a) Götze, H. J.; Sheldrick, W. S.; Siebert, A. F. M. *Fresenius J. Anal. Chem.* **1993**, *346*, 634−638. (b) Siebert, A. F. M.; Fröhling, C. D. W.; Sheldrick, W. S. *J. Chromatogr., A* **1997**, *761*, 115−127.
(35) (a) Adlhart, C.; Hinderling, C.; Baumann, H.; Chen, P. *J. Am. Chem. Soc.* **2000**, *122*, 8204−8214. (b) Wan, K. X.; Shibue, T.; Gross, M. L. *J. Am. Chem. Soc.* **2000**, *122*, 300−307. (c) Nemeth, J. F.; Hochensang, G. P., Jr.; Marnett, L. J.; Caprioli, R. M. *Biochemistry* **2001**, *40*, 3109−3116.
(36) Tomer, K. B. *Chem. Rev.* **2001**, *101*, 297−328.
(37) (a) Kratz, F.; Hartmann, M.; Keppler, B.; Messori, L. *J. Biol. Chem.* **1994**, *269*, 2581−2588. (b) Smith, C. A.; Sutherland-Smith, A. J.; Keppler, B. K.; Kratz, F.; Baker, E. N. *J. Biol. Inorg. Chem.* **1996**, 424−431. (c) Trynda-Lemiesz, L.; Keppler, B. K.; Kozlowski, H. *J. Inorg. Biochem.* **1999**, *73*, 123−128. (d) Messori, L.; Orioli, P.; Vullo, D.; Alessio, E.; Lengo, E. *Eur. J. Biochem.* **2000**, *267*, 1206−1213. (e) Piccioli, F.; Messori, L.; Orioli, P.; Keppler, B.; Alessio, E.; Sava, G. *J. Inorg. Biochem.* **2001**, *86*, 379−379.

Ru(II) complexes interact only weakly with transferrin (unpublished data). It seems likely, therefore, that the mechanism of action of ruthenium(II) arene anticancer complexes is different from that of ruthenium(III) complexes.

Acknowledgment. We thank the Royal Society (Royal China Fellowship for F.W.), CVCP (ORS award for H.C.), EPRSC, Wellcome Trust (Edinburgh Protein Interaction Centre), Wolfson Foundation, and ETF for their support of this work, and Sally Shirran for helpful advice on ESI-MS.

Supporting Information Available: NMR data for complexes **4a**, **4b**, **5**, and **6** (Table S1), schematic drawings of fragments observed by ESI-MS (Chart S1), and additional figures detailing characterization (Figures S1−S12). This material is available free of charge via the Internet at http://pubs.acs.org.

IC025538F